Article:
McArthur, AD orcid.org/0000-0002-7245-9465, Claussmann, B, Bailleul, J et al. (2 more authors) (2020) Variation in syn-subduction sedimentation patterns from inner to outer portions of deep-water fold and thrust belts: examples from the Hikurangi subduction margin of New Zealand. Geological Society, London, Special Publications, 490. pp. 285-310. ISSN 0305-8719

https://doi.org/10.1144/sp490-2018-95

Accepted Manuscript

Geological Society, London, Special Publications

Variation in syn-subduction sedimentation patterns from inner to outer portions of deep-water fold and thrust belts: examples from the Hikurangi subduction margin of New Zealand

Adam Daniel McArthur, Barbara Claussmann, Julien Bailleul, William McCaffrey & Alan Clare

DOI: https://doi.org/10.1144/SP490-2018-95

Received 14 May 2018
Revised 1 February 2019
Accepted 1 March 2019

Variation in syn-subduction sedimentation patterns from inner to outer portions of deep-water fold and thrust belts: examples from the Hikurangi subduction margin of New Zealand

A.D. McArthur [1*], B. Claussmann[2,3], J. Bailleul[2], A. Clare[4], W.D. McCaffrey[1]

1. School of Earth and Environment, University of Leeds, Leeds, LS2 9JT, United Kingdom
2. EA 7511, Basins-Reservoirs-Resources (B2R), Geosciences department, UniLaSalle, Beauvais, France
3. Schlumberger, Software Integrated Solutions, London, SW1E 6AJ, United Kingdom
4. OMV New Zealand Ltd, The Majestic Centre, 100 Willis Street, 6011 Wellington, New Zealand

* Correspondence (a.mcarthur@leeds.ac.uk)

Abstract

The structure and distribution of accommodation in fold and thrust belts is seen to vary both laterally and longitudinally. Here we integrate gravity, bathymetry and 2D seismic datasets to investigate the structural and stratigraphic variation in the southern part of the Hikurangi subduction wedge, onshore and offshore North Island, New Zealand. Three morphostructural portions are recognised:

- The inner portion demonstrates reactivation of inherited structures, producing thick-skinned deformation. Pre-subduction rocks are represented by kilometres of acoustically chaotic seismofacies. Thick-skinned deformation and readily deformable substrate leads to the development of wide trench-slope sub-basins, infilled with >5 km of syn-subduction sediments.

- The mid portion typically demonstrates thrust faults with connections to deeper structures, leading to the development of an imbricate system with asymmetrical sub-basins typically <5 km thick developed on the back-limb of thrust related folds.
- An antiformal stack marks the transition from the thick-skinned interior of the basin to the thin-skinned accretionary prism. Beyond this, the relatively non-deformed outer portion demonstrates frontal folds, propagating thrusts and up to 3 km thickness of syn-subduction strata.

Structural variation across the subduction wedge controls the generation of accommodation with implications for sediment distribution within fold and thrust belts and for petroleum system development. –END OF ABSTRACT-

The style and distribution of sediments in actively developing subduction wedges are fundamentally influenced by the underlying structural style, which may not conform to existing models of margin-scale structure in convergent settings (e.g. Morley *et al*. 2011). Lateral variation in fault and detachment fold evolution (e.g. Mahoney *et al*. 2017; Totake *et al*. 2017; Watkins *et al*. 2017), has major implications for the development, fill and subsequent deformation of submarine slope accommodation (e.g. Booth *et al*. 2003; Prather 2003; Kane *et al*. 2010; Olafiranye *et al*. 2013). As well as tectonism and eustasy, the flux, distribution and load of sediments also fundamentally influences the development of growth structures (e.g. Storti and McClay 1995; Grando and McClay 2007; Duerto and McClay 2009, 2011; Barrier *et al*. 2013: Noda 2018). Therefore, understanding the interaction of structural style and sedimentary pathways is essential for unravelling the distribution of petroleum systems within syn-kinematic intervals of deep-water fold and thrust belts, which are often considered prospective, e.g. Sabah, NW Borneo (Hesse *et al*. 2009).

Here we investigate the structural variation, resulting morphology and stratigraphic development of trench-slope sub-basins, with examples from the petroleum province of the Hikurangi subduction margin, being the East Coast Basin of New Zealand (Fig. 1). This study integrates gravity data, regional bathymetry and recently acquired 2D seismic data across the margin. This allows examination of not only the lateral, but also longitudinal and temporal variation in the structure and fill of trench-paralleling sub-basins. This margin displays a distinct bow shape (Fig. 1), which is also apparent in other subduction wedges, such as the Sinú (Vinnels *et al*. 2010) and the Makran (Grando and McClay 2007). This overall shape has previously been interpreted as the result of seamount subduction in the northern zone (Pecher *et al*. 2005) and of the change from oblique subduction to strike-slip deformation at the southern end (Nicol *et al*. 2007; Barnes *et al*. 2010; Fagereng 2011). The East Coast Basin has received extensive analysis using outcrop and vintage seismic data (e.g. Lewis and Bennett 1985; Davey *et al*. 1986; Lewis and Pettinga 1993; Barnes and Mercier de Lépinay 1997; Barnes *et al*. 2010; Bailleul *et al*. 2013; Burgreen-Chan *et al*. 2016). However, previous studies have been unable to resolve the full depth of the trench-slope sub-basins or the distribution of reflectors and their terminations within them, e.g. Barker *et al*. (2009).

The aim of this study is to investigate how variations in structural style influence the generation of accommodation and syn-subduction sedimentation patterns across an active subduction wedge. Specific objectives are to:

- Integrate regional gravity, bathymetry and 2D seismic datasets to define the structural variation both laterally and longitudinally along the southern part of the Hikurangi subduction margin.
- Refine the distribution and migration of the deformation and how it impacts the generation, structure and fill of trench-slope sub-basins.

- Develop a model for the variation in sedimentation styles across deep-water subduction wedges.
- Consider the implications for hydrocarbon prospectivity in deep-water fold and thrust belts on convergent margins.

Tectono-stratigraphic setting

The Hikurangi subduction complex has been developing over at least the last 25 Myr by oblique convergence of the oceanic Pacific Plate with the Australian Plate (Ballance 1976; Spörli 1980; Pettinga 1982; Chanier and Ferriere 1991; Field *et al*. 1997; Nicol *et al*. 2007; Reyners 2013). The wedge is buttressed to the west by a back-stop of Permian to Lower Cretaceous basement, known as the Torlesse Supergroup, which formed as part of an older accretionary complex on the south-eastern margin of Gondwana (Spörli 1978; Bradshaw 1989; Mortimer 2004; Mortimer et al. 2014). This supergroup comprises a series of terranes, with boundaries between terranes and the Mesozoic deformation fabric acting as strong controls on planes of weakness, which were subsequently re-activated during Cenozoic deformation (Cashman *et al*. 1992; Field *et al*. 1997; Furlong and Kamp 2009).

The collision of Zealandia with the Hikurangi Plateau, an area of thickened oceanic crust, resulted in a hiatus of the Gondwanan subduction around the Early to Late Cretaceous boundary (Bradshaw 1989; Davy *et al*. 2008; Reyners 2013). The basement is variably conformably or unconformably succeeded by Cretaceous, deep-marine sedimentary rocks, represented by the now significantly deformed Glenburn Formation and Tinui Group (Fig. 2; Johnston 1980; Chanier and Ferriere 1991; Field *et al*. 1997; Lee and Begg 2002). This Group includes the Upper Cretaceous to Paleocene marine sedimentary rocks of the Tangaruhe, Whangai and Waipawa Formations (Fig. 2), interpreted to represent a sustained period of tectonic quiescence, which was contemporaneous with the final break-up of

Gondwana and the opening of the Tasman Sea (Laird and Bradshaw 2004). Above the Waipawa Formation, which is a source rock in the East Coast Basin (Field *et al*. 1997; Hollis *et al*. 2005), sediments are dominated by smectitic mudstones of the Upper Paleocene to Eocene Wanstead Formation, and the Eocene to Oligocene Weber Formation marl (Fig. 2).

Hikurangi margin subduction began at *ca*. 25 Ma, resulting in the development of the Hikurangi subduction wedge and the Hikurangi Trough, which defines the eastern limit of the East Coast Basin (Fig. 1; Ballance 1976; Pettinga 1982; Chanier and Ferriere 1991; Field *et al*. 1997; Nicol *et al*. 2007; Barnes *et al*. 2010; Reyners 2013). During the Neogene the overriding Australian Plate underwent significant internal deformation in the form of ENE-WSW trending reverse, normal and strike-slip faulting, leading to the development of fold and thrust bounded, trench-slope sub-basins (Chanier *et al*. 1999; Bailleul *et al*. 2007; Nicol *et al*. 2007; Barnes *et al*. 2010; Reyners 2013).

Three main tectonic stages can be recognised since the onset of the current phase of subduction (Fig. 2; Wells 1989; Chanier and Ferriere 1991; Reyners 2013), related to the overriding plate's response to Pacific Plate subduction, comprising: 1) An early Miocene compressional stage, expressed by the ESE emplacement of nappes, folding and reverse faulting along the margin (Rait *et al*., 1991; Chanier *et al*., 1999; Bailleul *et al*., 2013). 2) A middle to late Miocene phase of mixed extension and compression. An extensional regime developed in the inner portion of the subduction wedge, with associated widespread subsidence and normal faulting, likely the result of gravitational collapse, which is attributed to tectonic erosion processes (Chanier *et al*. 1999; Barnes *et al*. 2002). The remainder of the wedge experienced continued compression as the deformation front moved outboard (Nicol *et al*. 2007; Furlong and Kamp 2009). 3) From the latest Miocene onwards a renewed basin-wide compression, expressed by further reverse faulting, thrusting and rapid Late Quaternary uplift, has resulted in the development of the present day fold and thrust belt (Nicol and Beavan 2003; Litchfield *et al*. 2007; Nicol *et al*. 2007; Bailleul *et al*. 2013; Jiao *et al*. 2017).

The Pliocene to recent history of the basin records significant uplift, due to acceleration of subduction (Nicol *et al*. 2007), resulting in the exhumation of the western, now onshore, part of the subduction wedge and development of the Coastal Ranges and the North Island axial ranges (Fig. 1; Ghani 1978 ; Beanland *et al*. 1998; Nicol *et al*. 2002; Litchfield *et al*. 2007; Nicol *et al*. 2007; Reyners *et al*. 2011; Trewick and Bland 2012). The region continues to experience deformation, although strain partitioning driven by oblique convergence has resulted in dominantly dextral strike-slip deformation onshore over the last million years (Beanland *et al*. 1998), with added complexity due to the onset of Taupo Volcanic Zone back-arc spreading (Acocella *et al*. 2003; Nicol and Wallace 2007).

Offshore, the subduction wedge is characterized by elongate, trench-parallel structures controlled by underlying thrust faulting and / or growing folds (Fig. 3; Lewis and Pettinga 1993; Barnes *et al*. 2010; Bailleul *et al*. 2013; Bland *et al*. 2015). Thrusts typically dip away from the trench (i.e. landward), whereas the associated folds are generally asymmetrical, with trench-ward vergence (Barnes et al. 1998). The subduction induced deformation has formed accommodation between structures, creating a series of trench-parallel, elongated sub-basins, with diachronous sedimentation patterns, which are punctuated by out of sequence thrusts and folds (Fig. 4; Chanier and Ferriere 1991; Bailleul *et al*. 2013). The fill of these sub-basins is complex, including widespread marine mudstones, turbidites, mass-transport complexes, and carbonates of the Miocene Palliser Group, the Pliocene Onoke Group and Pleistocene to recent sediments (Fig. 2; Lee and Begg 2002; Bailleul *et al*. 2013). A close interplay between tectonics and stratigraphy is apparent and the resulting sediments are punctuated by a series of unconformities (Neef 1992; Bailleul *et al*. 2007, 2013; Burgreen and Graham 2014; Burgreen-Chan *et al*. 2016).

Dataset and methodology

Multiple datasets have been integrated to study the margin scale variation in deformation and sedimentation in the southern part of the Hikurangi margin.

1) Satellite-derived Free-air (offshore) and crustal Bouguer gravity anomaly (onshore) data were provided by the Institute of Geological and Nuclear Sciences (GNS Science) of New Zealand (McCubbine *et al*. 2017). These were used to examine the crustal structure of the Hikurangi margin (Fig. 3A).

2) High resolution bathymetric data (100 m grid) were supplied by the National Institute of Water and Atmospheric Research, New Zealand (NIWA) to study the expression of active structures on the sea-floor, variation in sub-basin surface dimensions and sediment pathways between sub-basins (Fig. 3B). Onshore geology maps and digital elevation model were provided by GNS Science (Heron 2014).

3) The PEG14 2D seismic reflection dataset was collected by WesternGeco in 2014 and reprocessed in 2016. This survey constitutes 5242 line-kilometres across the southern part of the Hikurangi margin (Fig. 3B). Data were collected in a frequency range of 3 to 200 Hz and full stack data are depth converted. In this dataset, a downward decrease in acoustic impedance is represented by a trough (red), and a downward increase is represented by a peak (black). Data were interpreted using the Petrel E&P software platform. Major faults and structures were interpreted and regional surfaces were extrapolated from the survey. Two well ties enabled the base Pliocene to be picked relatively confidently (Fig. 1). Vintage data from publically available surveys IAE-1 and 05CM were also consulted for the near-shore structure; these are available courtesy of New Zealand Petroleum and Minerals (https://www.nzpam.govt.nz/maps-geoscience/).

Results: Architecture of the East Coast Basin

Gravity data

Gravity observations

Gravity data demonstrates positive anomalies in both emergent and submerged areas of the inner portion of the East Coast Basin, whilst the prospective, mid to outer portion of the basin shows neutral to negative anomalies (Fig. 3A). Some but not all ridges in the mid to outer portions, such as the Rock Garden and the Aorangi Ridge also show positive anomalies.

Gravity interpretations

The positive anomalies indicates that the inner portion may have developed over existing thickened crust (Henrys *et al*. 2013), whereas the outer portion could be developing over oceanic crust (Davy and Wood 1994; Reyners 2013). Some of the positive values in the inner portion may also be driven by anomalously thick units of Cretaceous to Paleocene rocks (K. Bland pers.com 2018). The positive anomalies associated with outer ridges indicate these are either sites of thickened crust, or of subducted seamounts, strings of which can be seen on the sea-floor approaching the trench (Fig. 3A).

Bathymetry and topography data

Bathymetry and topography data help define the morphology of the trench-parallel depocentres within the subduction wedge (Table 1). Distribution of accommodation is highly variable along strike, but may relate to underlying factors. Bathymetry and gravity data highlight variations in the morphology and allows division of the area into an inner portion, where the troughs are largely filled, a mid portion where troughs are filling and an outer portion, where the proto-troughs are developing (Fig. 3). Beyond this sits the Hikurangi Trough (Fig. 3B). In general, the bow shape of the margin is associated with significant variation in the distribution of structures and adjacent sub-basins (Fig. 3B). In the northern zone of the study area, the margin as measured from the North Island axial ranges to the active deformation front at 3 km water depth, is 190 km, giving an overall wedge taper of <1^{o}. The central zone displays the widest portion, being up to 227 km wide, giving a slope gradient of 0.76^{o}. The southern zone narrows and steepens considerably, being 43 km wide with a gradient of 4.0^{o}.

Topography observations

The onshore morphology is highly variable along strike. In the central zone of the emergent part of the inner wedge, located to the west of the North Island axial ranges, three main structural highs can be defined: the Puketoi Range, the Pongaroa Block and the Coastal Block (Fig. 3B). Between these ridges sit the Dannevirke, Puketoi and Akitio sub-basins (Table 1; Fig. 3B). To the north, a simpler configuration is seen, with the widening of the Dannevirke Sub-basin and the Makara Sub-basin (Table 1). In the southern zone, the Wairarapa Sub-basin is the dominant depocentre (Table 1), with only thin strips of syn-subduction strata preserved to the east of the Aorangi Range, primarily represented by the Whareama Sub-basin, (Fig. 3B; Table 1; Chanier and Ferriere 1991).

Topography interpretations

The Wairarapa and Dannevirke sub-basins represent the modern forearc basin to the North Island axial ranges (Cashman *et al*. 1992). The Akitio, Makara, Puketoi and Whareama sub-basins represent the preserved remnants of trench-slope sub-basins (Pettinga 1982; Bailleul *et al*. 2013). It is inferred that significantly more sediment was deposited; only erosional remnants remain, with isolated Neogene outliers (Lee *et al*. 2011).

Bathymetry observations

A range of trench-parallel ridges in shallow to deep-water are seen, separated by elongate troughs or sub-basins, typically tens of kilometres long by kilometres wide (Fig. 3).

In the submerged inner portion, the northern zone displays depressions such as the Motuokura Trough (Table 1; Fig. 3). Troughs in the inner portion largely show smooth surfaces, with minimal relief on ridges (typically < 100 m). The mid portion of the northern zone comprises a series of eight narrow troughs, each no more than 5 km wide, with steep ridges occurring in progressively deeper-water (Table 1; Fig. 3). These ridges and troughs are stacked behind the Rock Garden, which marks the transition to the outer portion of the wedge (Fig. 3B). The outer portion is more rugose than the inner portion, with ridges displaying up to 1 km of relief above adjacent troughs (Fig. 3). Ridges typically display an asymmetric profile with a gentler back-limb and steeper, trench verging fore-limb (Fig. 3 and 4). Beyond the Rock Garden sits the deformation front, followed by a 10 to 15 km wide proto-thrust zone and the Hikurangi Trough (Fig. 3).

The central zone of the submerged inner portion exhibits a subdued bathymetry; i.e. the Coastal Sub-Basin, the westernmost edge of which crops out along the coastline (Table 1; Fig. 3). The Madden Sub-basin is the exception, being incised by the Madden re-entrant (Table 1; Fig. 3). The mid portion of the wedge displays a number of subtle ridges, typically with less than 100 m elevation above adjacent troughs, typically less than 30 km long (Table 1; Fig. 3). In the outer wedge a series of three major ridges and adjacent sub-basins are seen and typically have a smooth top surface, with relief between ridges and troughs typically <300 m (Fig. 3). The majority of the central, outer troughs are narrow, being <7 km wide and no more than 60 km long (Table 1).

In the steep and narrow southern zone, the Pahaua Trough is the only evident depocentre in the inner portion (Table 1; Fig. 3). The mid portion is less than 15 km wide, tapering to the south where it is cut by transverse canyons (Fig. 3; Mountjoy *et al*. 2009) and only the Uruti Trough is apparent (Table 1). In the outer portion of the wedge only the Pukehoko and Aorangi troughs are apparent (Table 1). Ridges show significant elevation above the troughs, of almost 1 km in places (Fig. 3). Outboard of the Hikurangi Trough sits the Pegasus Basin (Fig. 1; Bland *et al*. 2015).

Bathymetry interpretations

Ridges are primarily interpreted to represent the sea-floor expression of convergence-related thrust-faults (Lewis and Pettinga, 1993). Variation in fault spacing is evident, but does not occur in a uniform fashion across the margin, with variation in sediment supply, efficiency of frontal accretion, topography of the subducting plate (including seamounts), out of sequence thrusting, obliquity of convergence and rate of convergence all contributing to the bow shaped margin (Lewis and Pettinga 1993; Pecher *et al*. 2005; Barnes *et al*. 2010). Therefore the size of adjacent troughs or sub-basins typically developed on the back-limb of ridges is not uniform across the margin, nor do they show a linear evolution towards the Hikurangi Trough (Table 1). Although now overfilled and in some cases being exhumed, the inner sub-basins are on average the widest and show greatest fault spacing, averaging 10-20 km width and 60-85 km length, probably because of strain localisation onto major faults (Bailleul *et al*. 2013). The mid portion demonstrates troughs 10-15 km wide by 70-100 km long, which appear filled to spill (Fig. 3). In the central zone, this fill and spill nature captures sediment in the outer troughs (McArthur and McCaffrey 2018), whereas in the southern and northern areas slope channels show connection with the Hikurangi Channel (Mountjoy *et al*. 2009). The outer troughs that are not bypassed are small, being 5-10 km wide and < 80 km long. The variation in fill is related to two factors: 1) The development of steeper and more persistent ridges in the northern and southern parts of the study area, and 2) the trapping of higher volumes of sediment in the central portion; the overfilled signature of which indicates significant trapping in intra-slope accommodation.

Seismic data

Subsurface data allow investigation of the effects of the variability in the structure and fill of sub-basins (Fig. 4, 5 and 6). Syn-subduction components show reflection terminations within the sub-basins, rather than simply being deformed in structures (Fig. 7). Five seismic units are defined within the syn-subduction interval (Table 2), allowing interpretation of regional syn-subduction surfaces and consideration of the lateral and longitudinal variation of structures, sub-basin geometries and their fill.

Northern zone, inner portion observations

High-angle, over-steepened thrust faults, often with associated back thrusts are imaged here (Fig. 7A). Major faults may connect with deep structures (Fig. 4). Reflectors within the structures often appears as seismic acoustic basement, occasionally with floating rafts of coherent reflectors (Fig. 7A). Sub-basins such as the Madden Sub-basin show over 5 km thickness to the base of the syn-subduction strata (Fig. 7A). Above a strong, coherent reflector much of the basal fill of the Madden Sub-basin is dominated by chaotic, seismic acoustic basement, however steeply dipping slabs of coherent reflectors can be seen on the edge of the Madden Banks, which show a general clockwise rotation towards the sub-horizontal unit D, where reflectors retain a strong degree of asymmetry towards the eastern margin (Fig. 7A).

Northern zone, inner portion interpretations

Major thrust faults are of a high angle implying they have experienced multiple stages of movement and are interpreted to show reactivation of pre-subduction structures. The seismic acoustic basement in the core of Madden Banks can be interpreted as the result of either: 1) Extreme deformation and / or development of vertical strata, preventing clear imaging of the structures. 2) Overpressure and remobilisation of the pre-subduction strata, as seen in the cores of onshore ridges with ductile claystones and marls of the Wanstead and Weber formations (Lee and Begg 2002). These features led Neef (1992) and Mazengarb (1998) to interpret the growth of shale diapirs in the onshore stratigraphy. Given that mud volcanoes have been reported on the sea-floor within the study area (Barnes *et al*. 2010) and that coherent strata can be seen at depth, below the chaotic interval (Fig. 7) the shale diapir interpretation is plausible. However a combination of the two is likely, producing reactivation zones (sensu Duerto and McClay 2009).

Northern zone, mid portion observations

Moving east, beyond the area of chaotic reflectors, a series of steeply dipping thrust faults that rarely break to surface can be seen, with associated roll-over anticlines (Fig. 4). Fault angles may be up to 50^{o} or greater in the upper 6 km of strata, but typically become less inclined with depth towards the sub-horizontal basal décollement (Fig. 4). These faults are associated with deep sub-basins, such as the Porangahau Trough (Fig. 7B). The Porangahau Trough shows coherent reflectors to over 9 km depth, however the first reflectors showing terminations within the trough are interpreted at 4.75 km depth (syn-subduction unit A). However, almost 2 km of the lower fill is composed of chaotic blocks (Fig. 7B). Initially the overlying reflectors of units C and D show a relatively even distribution, pinching out towards both margins, however unit E shows an asymmetry of reflectors, stepping to the east (Fig. 7B).

Northern zone, mid portion interpretations

This area of steep thrust faults, originating on the primary décollement and producing associated detachment fold anticlines can be interpreted as an imbricate fan, with a series of sub-basins developing on the back limbs (e.g. Grando and McClay 2007). Imbricate fans occur where a series of imbricated thrust faults branch out of a single, deeper basal detachment (Van Der Pluijm and Marshak 2004). Therefore, these sub-basins are not piggyback basins, but are relatively fixed areas of intra-slope accommodation. Reflectors of the syn-subduction units pinch out against the margins of the trough, in contrast to the pre-subduction reflectors that are deformed and truncated by growth structures. The thickness of syn-subduction strata observed in these sub-basins implies that significant volumes of sediment were delivered to the Porangahau Trough, but that until recently subsidence was outpacing sedimentation. The initial fill may principally be composed of remobilised sediment, forming mass-transport complexes (MTCs), as seen in the basal infill of the outcropping sub-basins (Bailleul *et al*. 2007).

Northern zone, outer portion observations

Here, a series of developing thrusts are imaged, with associated fault propagation folds, some of which have developed into detachment folds, i.e. the Akitio Ridge (Fig. 7D). Within this portion, relatively coherent strata are being dissected, but can typically be traced across fault blocks, e.g. either side of the Akitio Ridge (Fig. 4). The Akitio Trough is main depocentre and shows continuous stratigraphy to c.8 km depth (Fig. 4), however the first discontinuous reflectors occur at 5 km depth (Fig. 7D), after which Reflectors remain relatively symmetrical. Continuing outboard, a large knoll is seen on the subducting plate, with thin cover over the subducting plate (Fig. 4).

Northern zone, outer portion interpretations

The outer portion of the wedge corresponds to the accretionary prism *sensu stricto*, which displays multiple detachments and detachment folds, but with relatively non-deformed sequences of reflectors (Fig. 4). Unlike the inner and mid portions, distinct segments of coherent reflectors are detaching from the subducting plate and being accreted to the front of the subduction wedge (Fig. 4). This contrasts to previous interpretations of the entire wedge representing an accretionary prism. The Akitio Trough demonstrates a distinctive evolution from coherent but deformed reflectors, truncated by thrusts to reflectors that terminate within the trough (Fig. 7D). This evolution is interpreted to represent the transition of this depocentre from accreted strata, previously deposited in the trench, to a trench-slope sub-basin.

Central zone, inner portion observations

Above the primary décollement, a mounded feature 50 km wide dominates the central zone of the study area, above which strata thin considerably (Fig. 5). Overlying reflectors are often incoherent, apart from rare floating intervals of coherent reflectors, such as those at 4 km depth below the well Titihaoa-1 (Fig. 8A). This interval is affected by numerous high-angle thrusts, which dissect the syn-subduction strata (Fig. 8A). Where resolvable, reflectors in the Coastal Sub-basin are seen to be relatively symmetrical, onlapping the Titihaoa Ridge until those of Unit C, which are seen to prograde over the top of the ridges (Fig. 8A). The uppermost reflector sequence demonstrates reflectors dipping and terminating landwards (Fig. 8A).

Central zone, inner portion interpretations

The large mounded feature at depth is interpreted as seismic acoustic basement, over-thickened due to subduction of a seamount, with chains of such features seen to be approaching the subduction wedge (Fig. 3; Barnes *et al*. 2010). Gravity data also add weight to an interpretation of thick-skinned deformation in the inner portion of the subduction wedge (Fig. 3). The nature of the reflectors of the seismic acoustic basement above the subducted seamount is interpreted to be the result of high-angle thrusts and potential remobilisation of pre-subduction sediment. The landward stepping reflectors that cap the sequence are interpreted as contourite drifts (sensu Faugères *et al*. 1999).

Central zone, mid portion observations

Beyond the inner area of limited accommodation thrusts become less regularly spaced, lower angle and don't penetrate to the seafloor (Fig. 3 and 5). Here the subducting plate shows a rugose surface. Deformation is creating the Uruti Trough (Fig. 3), within which syn-subduction reflectors up to 3 km thick are initially symmetrical, however the upper units D and E show asymmetry (Fig. 8B).

Central zone, mid portion interpretations

Sandwiched between the highly deformed inner and outer portions, limited accommodation is present. This is potentially due to the subduction of a seamount (Fig. 5), leading to high deformation and limited generation of accommodation. High sedimentation rates have potentially allowed the continued development of the Uruti Trough (Noda 2018).

Central zone, outer portion observations

Outboard of the Uruti Trough a complex 10 km wide deformation zone shows numerous detachments and steep thrust faults, beyond which a series of thrusts with detachment folds are developing (Fig. 5). A distinction can be made between accreted strata, which are deformed by folds and / or truncated by faults and the fill of slope accommodation, such as the Aorangi Trough (Fig. 8D). This trough shows distinct asymmetry in its upper 1 km, with reflectors thinning toward and pinching out against the Aorangi Ridge, whereas reflectors of Unit C and below show deformation but continuity through the developing structures (Fig. 8C).

Central zone, outer portion interpretations

The subduction of a seamount has restricted the development of an imbricate fan and an antiformal stack has formed, which marks the transition from thick to thin-skinned deformation (Fig. 5). Beyond this area of intense deformation a frontal fold area is evolving, where the majority of reflectors represent sediment deposited on the subducting plate and are now being accreted (Lewis and Pettinga 1993; Barnes *et al*. 2018). Minor accommodation is actively developing on the back limbs of thrusts. The outer portion is interpreted as the true accretionary prism of the larger subduction wedge.

Southern zone, inner portion observations

A very narrow and heavily deformed inner portion of the subduction wedge is seen in vintage seismic data in the southern zone, as described by Bland *et al*. (2015). Many high-angle thrusts are imaged, but reflectors are often chaotic, appearing as seismic acoustic basement. Well-developed slope accommodation is not apparent (see the NW area of Figure 9 in Bland *et al*. 2015).

Southern zone, inner portion interpretations

As with the central and northern zones, the inner portion exhibits high-angle thrusts combined with seismic acoustic basement. Therefore, this portion is interpreted as a reactivation zone, where deformation is focused on a small number of large faults, promoting limited development of accommodation (Bland *et al.* 2015).

Southern zone, mid portion observations

A series of sub-vertical, out-of-sequence thrusts, with detachment folds are developing towards the Pukehoko Ridge (Fig. 6). This ridge demonstrates a series of thrusts that are detaching and coalescing to elevate the ridge 1 km higher than the adjacent trough (Fig. 9). This has provided limited accommodation, with only the Pukehoko Trough apparent as a major depocentre, reflectors within which are relatively symmetrical (Fig. 9).

Southern zone, mid portion interpretations

Here we interpret an imbricate fan culminating in a proto-antiformal stack. Other than relatively recent reflectors prograding over the wedge, sediments have been concentrated into the Pukehoko Trough or were bypassed via slope canyons (Mountjoy *et al.* 2009), with relatively symmetrical reflectors implying this trough has been starved of sediment through its fill. The restricted size of the imbricate fan in the southern zone is interpreted as a result of the transition from subduction to oblique strike-slip deformation at the southern end of the margin (Nicol *et al.* 2007).

Southern zone, outer portion observations

Beyond the Pukehoho Ridge, deformation is largely limited to broad folds that can be seen in the trench (Fig. 9). Almost 5 km of syn-subduction strata are imaged in the trench, with a series of coherent reflector units thinning towards and truncating against the Chatham Rise (Fig. 9). Southern zone, outer portion interpretations

Here we interpret a frontal fold system to be developing and deforming reflectors of the trench sequence (Lewis and Pettinga 1993). Flexure of the subducting plate, with associated plate bending normal faults provided accommodation for a significant thickness of syn-subduction strata, which continues to thicken south into the Pegasus Basin (Bland *et al.* 2015). A minimal volume of material is being accreted here, with the outer portion being heavily deformed and less than 10 km wide.

Discussion

Lateral and longitudinal evolution of basin structure as a control on the distribution and type of intra-slope accommodation

The dimensions of ridges and sub-basins are seen to vary both laterally and longitudinally across the subduction wedge (Table 1). This allows the definition of three portions, from the outcropping inner to the submerged outer portion of the subduction wedge, which also show north-to-south variation along the margin (Table 3). In the inner portion of the subduction wedge, sub-basins are very deep, being up to 5 km thick, show distinct asymmetry and exhibit a complex and deformed fill (Fig. 7B and 8B).

Several mechanisms can be proposed to explain the thickness and complexity of the fill of the inner sub-basins. Being in the inner portion of the wedge, these inner sub-basins are the oldest and have undergone the most deformation (Bailleul *et al*. 2013 and references within). Faulting is longest lived here and outcropping faults have multiple phases and styles of motion (Malie *et al*., 2017). Deformation that has become focused on major structures may also drive continued subsidence of adjacent sub-basins, which also show repeated activity of sub-basin bounding faults by continued MTC development (Fig. 7B). Furthermore, if the seismic acoustic basement identified in the pre-subduction reflectors truly represents mobile substrate, then this may be pushed away from sites of deposition, where loading of sediments has occurred, hence further deepening the inner sub-basins (e.g. Wu and Bally 2000; Morley *et al*. 2011). Regardless, the inner sub-basins represent true trench-slope sub-basins, rather than accreted and subsequently deformed trench floor material (Fig. 10). This is seen within the outcropping sub-basins, where the initial syn-subduction strata are accompanied by mass-wasting products; sea-floor relief is required to generate such MTCs (Bailleul *et al*., 2007).

The mid portion of the wedge displays high-angle thrust bounded sub-basins, up to 4.75 km thick. The lower fill of these sub-basin appears relatively symmetrical, but evolves to an asymmetric fill in the upper portions of sub-basins (e.g. Fig 7C). This could reflect the transition from the creation of trench-slope sub-basins, in which sediments were contained on the back-limbs of developing detachment folds, whereas continued propagation of the thrusts lead to faults defining the sub-basin geometry and asymmetric fill. This portion of the subduction wedge, here classed as an imbricate fan, represents material that has always been accumulating in trench-slope sub-basins, rather than being previously accreted from material deposited in the trench (Fig. 11).

In contrast, the outer portion of the subduction wedge demonstrates sections of accreted sea-floor and only recently developed detachment fold related depocentres associated with the frontal fold area (Barnes and Mercier de Lépinay 1997; Ghisetti *et al*. 2016; Barnes *et al*. 2018). The outer portion is characterized by isolated depocentres, typically with less than 1 km of syn-subduction sediment fill (e.g. Fig. 8D). These proto-trench-slope sub-basins do not show significant intra-sub-basin deformation, compared to the more developed inner to mid sub-basins. Whether slope sediments represent accreted material or true trench-slope sub-basins has significant implications for their sedimentary fill and the distribution of sediment across active margins. Trench-slope sub-basins demonstrate complex reflector packages, representing the various stages of syn-subduction development (Table 2; Fig. 7). The reflector geometries within trench-slope sub-basins may represent intra-slope turbidite systems (Bailleul *et al*., 2007) with portions of the fill characterised as MTCs, whereas accreted material displays much simpler reflector geometries that do not indicate sustained sediment supply (Fig. 7 H-J). Such strata are likely mud-rich, other than in areas proximal to the trench-axial channels (Fig. 10).

Therefore, assumptions regarding the style, age and sediment flux must be carefully considered for each portion of a subduction wedge; it is not a case of relatively uniform deposition across an area that has subsequently been deformed. This genetic variation in the dimensions and subsequent fill of sub-basins may also apply to other subduction margins, for example the Makran (Grando and McClay 2007) and the Sinú (Vinnels *et al*. 2010), which may require re-evaluation of their stratigraphic evolution. This generic insight may help in prediction of the distribution of accommodation and its fill in other subduction wedges (Fig. 10).

Suitability of inner, outcropping sub-basins as analogues for outboard sub-basins

In the absence of well data or other information regarding the fill of the offshore sub-basins, the outcropping sub-basins provide our best insights into the stratigraphic evolution of the trench-slope depocentres (Bailleul *et al*. 2007; Burgreen and Graham 2014). However, given the variation in sub-basin structure and apparent reflector styles across the wedge, the uncritical use of the inner, outcropping sub-basins as analogues for the offshore sub-basins is questionable. This is particularly true when comparing the outer portion, which exhibits accretion of sediments previously deposited in the trench. The submerged inner sub-basins imaged that display multiple angular unconformities and a heterolithic fill are most comparable to the outcropping systems (Fig. 10). However, some obvious variations in the stratal evolution of the outcropping sub-basins exist when compared to the subsurface inner sub-basins. A principal difference is the occurrence of shallow-marine strata in the Akitio Sub-basin (Bailleul *et al*. 2007). Only the uppermost fill of the next sub-basin outboard shows the presence of shallow-marine strata (Bailleul *et al*. 2013) and no obvious shallow-marine reflector geometries e.g. prograding clinoforms, were observed in the offshore dataset beyond the present shelf break (e.g. Fig. 4).

A general trend may exist with the innermost, outcropping sub-basins interpreted to represent the oldest, most mature portion of the subduction wedge (Bailleul *et al*. 2013). As such, the full range of stratal elements documented onshore may only be partially developed in the evolving, outboard sub-basins. The initial fill of the mid portion trench-slope sub-basins displays significant MTC development (e.g. Fig. 7F) and subsequently shows relatively symmetrical fill with reflectors pinching out to sub-basin margins, which may reflect an early, fully ponded stage of sub-basin fill. Subsequent development of asymmetrical reflectors may represent less confined sedimentation as the accommodation is filled. However, this may only hold true for the inner depocentres that have always been trench-slope systems, rather than sub-basins developing over the frontal folds, which display much simpler reflector packages (Fig. 8G).

Sub-basins in the northern and southern zones of the study area show simpler fills, which may represent the relatively sediment starved nature of these higher slope gradient regions e.g. the Pukehoko Trough (Fig. 9). Here, major transverse channels can be seen to completely bypass the slope system, with sediment fed into Hikurangi Channel, even at present sea-level (Mountjoy *et al*. 2018). Conversely, in the central, lower taper zone of the wedge, where the imbricate fan is best developed, we observe a fill and spill hierarchy (Fig. 7; McArthur and McCaffrey 2018). This may be due to the underlying structure, but also a feedback mechanism of sedimentary loading enhancing the generation of accommodation (Storti and McClay 1995).

Implications for hydrocarbon exploration of subduction wedges

The variation in accommodation and hence stratigraphic architecture has implications for the prospectivity of subduction wedges. Although the inner sub-basins display the most stratigraphic heterogeneity, they also display the greatest structural complexity (Fig. 4). Imaging of trapping structures here is difficult, leading to significant exploration uncertainty. Long offset seismic data acquisition is essential to have any chance of imaging over-steepened and reactivated thrusts. Development of significant overpressure also highlights the risk of exploring the innermost portion of the wedge (Uruski 1997), which caused both offshore wells to be prematurely abandoned. Furthermore, if sedimentation in the inner portion has always been within trench-slope sub-basins, then any deep-water reservoirs will be contained within the troughs, rather than developing over structural highs, as might be the case for accreted strata (Fig. 10). This was seen in the Titihaoa-1 well, which only encountered thin-bedded turbidites at the sub-basin margin.

Reflectors within the trench appear to lack distinctive geometries that might support the development of suitable reservoirs in this area, other than possible expressions of the palaeo-Hikurangi Channel (Bland *et al.* 2015). However, unless abandoned by major avulsion, deeper portions of this axial channel would present a leakage risk through younger channel deposits to the modern, sea-floor channel. No evidence of dissection and incorporation of older parts of the trench-axial channel into the accretionary prism has been observed.

Therefore, the thrust bounded sub-basins in the mid portion of the subduction wedge appear to represent the most prospective area, particularly those that display deformation associated with detachment folds. For example in the central zone of the Hikurangi subduction wedge the thickness and the distinctive reflector geometries of the syn-subduction interval are similar to the reservoir analogues described at outcrop (Bailleul *et al.* 2007); prospectivity may be enhanced where intra-slope reservoirs were inverted to produce trapping structures prior to hydrocarbon charge.

Conclusions

New data have allowed improved resolution of the Hikurangi margin subduction wedge, with the true extent of trench-slope sub-basins on this convergent margin being revealed. Significant variation in the structure of the margin has resulted in the development of a variety of accommodation and sediment distribution styles. Although there are longitudinal variations, a broad inboard-to-outboard subdivision of the wedge can be made. Key elements include:

1. An inner portion, within which reactivation of pre-subduction structures promotes thick-skinned deformation. Pre-subduction rocks in this inner portion are represented by kilometres of acoustically chaotic, potentially mobile substrate, within and below which are coherent reflectors packages. The thick-skinned deformation and presence of mobile strata has led to the development of wide trench-slope sub-basins, infilled with syn-subduction sediments that may exceed 5 km in thickness. Neogene sediments accumulated here have always been contained in the slope system, rather than representing accreted trench material.

2. A mid portion, beyond the modern shelf-slope break that typically demonstrates out-of-sequence thrust faulting with connections to a basal décollement. This primary décollement represents the modern subduction interface between the Australian and Pacific plates. Imbricate fan thrusts sole-out upon this surface; where asymmetrical sub-basins typically <5 km thick have developed on the back-limbs of major thrust related folds. Here reflectors remain coherent and may show continuity and evolution from a relatively unconfined pre-subduction configuration.

3. An outer portion, which is marked by an antiformal stack, beyond which the modern day accretionary prism *sensu stricto* is developing. A transition is seen from reflectors representing sediments that were previously deposited in the trench and subsequently accreted, to those representing units that onlap growth structures and are contained within developing trench-slope sub-basins, which may be up to 3 km thick.

Further outboard up to 5 km thickness of syn-subduction strata have accumulated on the trench floor, within which rotations and terminations associated with thrust propagation and frontal fold development allow inference of the evolution of this sector of the margin.

Contrary to previous interpretations, the extent of the actively accreting portion of the margin is restricted to the outboard 10 to 40 km of the wider subduction wedge. Neogene sediments of the inner and mid portions of the wedge have always been confined within the slope system.

This study confirms that sedimentation styles are highly variable across the Hikurangi margin. Underlying structures control the development of distinctive types of accommodation, degree of sediment flux and stratigraphic evolution from relatively complex inboard portions of the subduction wedge towards the simple relfectors of the trench-slope terminus. Therefore, basin fill across convergent margins may not be uniform or readily predictable and attempts to characterise the lateral and longitudinal variation in structure and resulting patterns of sedimentation is required. Understanding such complexity is essential to unlock the potential of deep-water fold and thrust belts, particularly in frontier exploration areas.

Acknowledgements

This research is funded by an ongoing JIP between Chevron, Equinor, OMV and Schlumberger. WesternGeco, Schlumberger, GNS Science and NIWA are thanked for permission to publish data. Schlumberger is thanked for an academic licence for use of the Petrel E&P software platform. Alex Wunderlich, Alex Karvelas, Lorna Strachan, Javier Tamara and Ken McClay are thanked for thoughtful insights. Kyle Bland and an anonymous reviewer are thanked for their helpful comments and Editor Michael Cottam for handling the manuscript.

References

Acocella, V., Spinks, K., Cole, J., and Nicol, A., 2003, Oblique back arc rifting of Taupo Volcanic zone, New Zealand: Tectonics, v. 22.

Bailleul, J., Robin, C., Chanier, F., Guillocheau, F., Field, B., and Ferriere, J., 2007, Turbidite Systems in the Inner Forearc Domain of the Hikurangi Convergent Margin (New Zealand): New Constraints on the Development of Trench-Slope Basins: Journal of Sedimentary Research, v. 77, p. 263–283, doi: 10.2110/jsr.2007.028.

Bailleul, J., Chanier, F., Ferrière, J., Robin, C., Nicol, A., Mahieux, G., Gorini, C., and Caron, V., 2013, Neogene evolution of lower trench-slope basins and wedge development in the central hikurangi subduction margin, new zealand: Tectonophysics, v. 591, p. 152–174, doi: 10.1016/j.tecto.2013.01.003.

Ballance, P.F., 1976, Evolution of the Upper Cenozoic magmatic arc and plate boundary in northern New Zealand: Earth and Planetary Science Letters, v. 28, p. 356–370.

Barker, D.H., Sutherland, R., Henrys, S., and Bannister, S., 2009, Geometry of the Hikurangi subduction thrust and upper plate, North Island, New Zealand: Geochemistry, Geophysics, Geosystems, v. 10, p. 1-23.

Barnes, P.M., and Mercier de Lepinay, B.M., 1997, Rates and mechanics of rapid frontal accretion along the very obliquely convergent southern Hikurangi margin , New

Zealand: Journal of Geophysical Research, v. 102, p. 24,931-24,952, doi: 10.1029/97JB01384.

Barnes, P.M., Mercier de Lépinay, B., Collot, J.Y., Delteil, J. and Audru, J.C., 1998, Strain partitioning in the transition area between oblique subduction and continental collision, Hikurangi margin, New Zealand: Tectonics, v. 17, p. 534–557.

Barnes, P.M., Nicol, A., and Harrison, T., 2002, Late Cenozoic evolution and earthquake potential of an active listric thrust complex above the Hikurangi subduction zone, New Zealand: Geological Society of America Bulletin, v. 114, p. 1379-1405.

Barnes, P.M., Lamarche, G., Bialas, J., Henrys, S., Pecher, I., Netzeband, G.L., Greinert, J., Mountjoy, J.J., Pedley, K., and Crutchley, G., 2010, Tectonic and geological framework for gas hydrates and cold seeps on the Hikurangi subduction margin, New Zealand: Marine Geology, v. 272, p. 26–48, doi: 10.1016/j.margeo.2009.03.012.

Barnes, P.M., Ghisetti, F.C., Ellis, S., and Morgan, J.K., 2018, The role of protothrusts in frontal accretion and accommodation of plate convergence, Hikurangi subduction margin, New Zealand: Geosphere, v. 14, p. 440-468.

Barrier, L., Nalpas, T., Gapais, D., and Proust, J.-N., 2013, Impact of synkinematic sedimentation on the geometry and dynamics of compressive growth structures: Insights from analogue modelling: Tectonophysics, v. 608, p. 737–752, doi: 10.1016/j.tecto.2013.08.005.

Beanland, S., Melhuish, A., Nicol, A., and Ravens, J., 1998, Structure and deformational history of the inner forearc region, Hikurangi subduction margin, New Zealand: New Zealand Journal of Geology and Geophysics, v. 41, p. 325–342, doi: 10.1080/00288306.1998.9514814.

Bland, K.J., Kamp, P.J.J., Pallentin, A., Graafhuis, R., Nelson, C.S., and Caron, V., 2004, The early Pliocene Titiokura Formation: Stratigraphy of a thick, mixed carbonate-siliciclastic shelf succession in Hawke's Bay Basin, New Zealand: New Zealand Journal of Geology and Geophysics, v. 47, p. 675–695.

Bland, K.J., Uruski, C.I., and Isaac, M.J., 2015, Pegasus Basin, eastern New Zealand: A stratigraphic record of subsidence and subduction, ancient and modern: New Zealand Journal of Geology and Geophysics, v. 58, p. 319–343.

Booth, J.R., Dean, M.C., DuVernay, A.E., and Styzen, M.J., 2003, Paleo-bathymetric controls on the stratigraphic architecture and reservoir development of confined fans in the Auger Basin: central Gulf of Mexico slope: Marine and Petroleum Geology, v. 20, p. 563–586, doi: 10.1016/j.marpetgeo.2003.03.008.

Bradshaw, J.D. 1989, Cretaceous geotectonic patterns in the New Zealand region: Tectonics, v. 8, p. 803-820.

Burgreen, B., and Graham, S., 2014, Evolution of a deep-water lobe system in the Neogene trench-slope setting of the East Coast Basin, New Zealand: Lobe stratigraphy and architecture in a weakly confined basin configuration: Marine and Petroleum Geology, v. 54, p. 1–22, doi: 10.1016/j.marpetgeo.2014.02.011.

Burgreen-Chan, B., Meisling, K.E., and Graham, S., 2016, Basin and petroleum system modelling of the East Coast Basin, New Zealand: a test of overpressure scenarios in a convergent margin: Basin Research, v. 28, p. 536–567, doi: 10.1111/bre.12121.

Cape, C.D., Lamb, S.H., Vella, P., Wells, P.E., and Woodward, D.J., 1990, Geological structure of Wairarapa Valley, New Zealand, from seismic reflection profiling: Journal of the Royal Society of New Zealand, v. 20, p. 85–105, doi:

10.1080/03036758.1990.10426734.

Carter, R.M., Carter, L., and McCave, I.N., 1996, Current controlled sediment deposition from the shelf to the deep ocean: the cenozoic evolution of circulation through the SW pacific gateway: Geologische Rundschau, v. 85, p. 438–451, doi: 10.1007/BF02369001.

Cashman, S.M., Kelsey, H.M., Erdman, C.F., Cutten, H.N.C., and Berryman, K.R., 1992, Strain Partitioning between structural domains in the forearc of the Hikurangi Subduction Zone, New Zealand: Tectonics, v. 11, p. 242–257, doi: 10.1029/91TC02363.

Chanier, F., and Ferriere, J., 1991, From a passive to an active margin; tectonic and sedimentary processes linked to the birth of an accretionary prism (Hikurangi Margin, New Zealand): Bulletin de la Société géologique de France, v. 162, p. 649–660.

Chanier, F., Ferrière, J., and Angelier, J., 1999, Extensional deformation across an active margin, relations with subsidence, uplift, and rotations: The Hikurangi subduction, New Zealand: Tectonics, v. 18, p. 862–876, doi: 10.1029/1999TC900028.

Davey, F.J., Hampton, M., Childs, J., Fisher, M.A., Lewis, K.B. and Pettinga, J.R.1986. Structure of a growing accretionary prism, Hikurangi margin, New Zealand: Geology, v. 14, p. 663-666.

Davy, B., and Wood, R., 1994, Gravity and magnetic modelling of the Hikurangi Plateau: Marine Geology, v. 118, p. 139–151, doi: 10.1016/0025-3227(94)90117-1.

Davy, B., Hoernle, K., and Werner, R., 2008, Hikurangi Plateau: Crustal structure, rifted formation, and Gondwana subduction history: Geochemistry, Geophysics, Geosystems, v. 9.

Duerto, L., and McClay, K., 2009, The role of syntectonic sedimentation in the evolution of doubly vergent thrust wedges and foreland folds: Marine and Petroleum Geology, v. 26, p. 1051–1069, doi: https://doi.org/10.1016/j.marpetgeo.2008.07.004.

Duerto, L., and McClay, K., 2011, Role of the shale tectonics on the evolution of the Eastern Venezuelan Cenozoic thrust and fold belt: Marine and Petroleum Geology, v. 28, p. 81–108, doi: https://doi.org/10.1016/j.marpetgeo.2009.11.005.

Fagereng, Å., 2011, Wedge geometry, mechanical strength, and interseismic coupling of the Hikurangi subduction thrust, New Zealand: Tectonophysics, v. 507, p.26-30.

Faugères, J.-C., Stow, D.A. V, Imbert, P., and Viana, A., 1999, Seismic features diagnostic of contourite drifts: Marine Geology, v. 162, p. 1–38.

Field, B.D., Uruski, C.I., and Institute of Geological & Nuclear Sciences, 1997, Cretaceous-Cenozoic geology and petroleum systems of the East Coast region, New Zealand: Institute of Geological & Nuclear Sciences.

Furlong, K.P., and Kamp, P.J.J., 2009, The lithospheric geodynamics of plate boundary transpression in New Zealand: Initiating and emplacing subduction along the Hikurangi margin, and the tectonic evolution of the Alpine Fault system: Tectonophysics, v. 474, p. 449–462, doi: 10.1016/j.tecto.2009.04.023.

Ghani, M.A., 1978, Late Cenozoic vertical crustal movements in the southern North Island, New Zealand: New-Zealand Journal of Geology and Geophysics, v. 21, p. 117–125, doi: 10.1080/00288306.1978.10420728.

Ghisetti, F.C., Barnes, P.M., Ellis, S., Plaza-Faverola, A.A., and Barker, D.H.N., 2016, The last 2 Myr of accretionary wedge construction in the central Hikurangi margin (North Island, New Zealand): Insights from structural modeling: Geochemistry, Geophysics, Geosystems, v. 17, p. 2661–2686, doi: 10.1002/2016GC006341.Received.

Grando, G., and McClay, K., 2007, Morphotectonics domains and structural styles in the Makran accretionary prism, offshore Iran: Sedimentary Geology, v. 196, p. 157–179, doi: https://doi.org/10.1016/j.sedgeo.2006.05.030.

Henrys, S., Wech, A., Sutherland, R., Stern, T., Savage, M., Sato, H., Mochizuki, K., Iwasaki, T., Okaya, D., Seward, A., Tozer, B., Townend, J., Kurashimo, E., Iidaka, T., *et al*., 2013, SAHKE geophysical transect reveals crustal and subduction zone structure at the southern Hikurangi margin, New Zealand: Geochemistry, Geophysics, Geosystems, v. 14, p. 2063–2083, doi: 10.1002/ggge.20136.

Heron, D.W. (custodian), 2014, Geological map of New Zealand 1:250,000. Lower Hutt, NZ: GNS Science. GNS Science geological map 1. 1 CD.

Hesse, S., Back, S., and Franke, D., 2009, The deep-water fold-and-thrust belt offshore NW Borneo: Gravity-driven versus basement-driven shortening: Geological Society of America Bulletin, v. 121, p. 939–953.

Hollis, C.J., Manzano-Kareah, K., Crampton, J., Field, B., Funnell, R., Morgans, H., and Rogers, K., 2005, Source rock potential of the East Coast Basin (central and northern regions): Ministry of Economic Development petroleum report, v. 3179, p. 1–156.

Jiao, R., Herman, F., and Seward, D., 2017, Late Cenozoic exhumation model of New Zealand: Impacts from tectonics and climate: Earth-Science Reviews, v. 166, p. 286–298, doi: https://doi.org/10.1016/j.earscirev.2017.01.003.

Johnston, M.R., 1980, Geology of the Tinui-Awatoitoi district, New Zealand. New Zealand Geological Survey Bulletin v. 94, pp. 60.

Joseph, L.H., Rea, D.K., and Van Der Pluijm, B.A., 2004, Neogene history of the Deep Western Boundary Current at Rekohu sediment drift, Southwest Pacific (ODP Site

1124): Marine Geology, v. 205, p. 185–206, doi: 10.1016/S0025-3227(04)00023-4.

Kane, I.A., Catterall, V., McCaffrey, W.D., and Martinsen, O.J., 2010, Submarine channel response to intrabasinal tectonics: The influence of lateral tilt: AAPG bulletin, v. 94, p. 189–219.

Laird, M.G., and Bradshaw, J.D., 2004, The break-up of a long-term relationship: the Cretaceous separation of New Zealand from Gondwana: Gondwana Research, v. 7, p. 273–286.

Lee, J.M. and Begg, J.G., 2002, Geology of the Wairarapa area: Lower Hutt, NZ: GNS Science.

Lee, J.M., Bland K., Townsend, D.B., and Kamp, P.J.J., 2011, Geology of the Hawke's Bay area: scale 1:250,000 : Lower Hutt, NZ: GNS Science.

Lewis, K. B. Bennett, D. J., 1985, Structural pattems onthe Hikurangi Margin: An interpretation of new seismic data, *in* Lewis, K.B. ed., New seismic profiles, cores, and dated rocks from the Hikurangi Margin, New Zealand. New Zealand oceanographic field report, v. 22, p. 3-25.

Lewis, K.B., and Pettinga, J.R., 1993, The emerging, imbricate frontal wedge of the Hikurangi margin: Sedimentary basins of the world, v. 2, p. 225–250.

van der Lingen, G., and Pettinga, J.R., 1980, The Makara Basin: a Miocene slope-basin along the New Zealand sector of the Australian-Pacific obliquely convergent plate boundary: Sedimentation in Oblique-slip Mobile Zones (Special Publication 4 of the IAS), v. 34, p. 191-215.

Litchfield, N., Ellis, S., Berryman, K., and Nicol, A., 2007, Insights into subduction-related uplift along the Hikurangi Margin, New Zealand, using numerical modeling: Journal of Geophysical Research: Earth Surface, v. 112, p. 1–17, doi: 10.1029/2006JF000535.

Mahoney, L., Hill, K., McLaren, S., and Hanani, A., 2017, Complex fold and thrust belt structural styles: Examples from the Greater Juha area of the Papuan Fold and Thrust Belt, Papua New Guinea: Journal of Structural Geology, v. 100, p. 98–119.

Malie, P., Bailleul, J., Chanier, F., Toullec, R., Mahieux, G., Caron, V., Field, B., Mählmann, R.F., and Potel, S., 2017, Spatial distribution and tectonic framework of fossil tubular concretions as onshore analogues of cold seep plumbing systems, North Island of New Zealand: Bulletin de la Société géologique de France, v. 188, pp. 24.

Mazengarb, C., 1998, Late Neogene structural development of Eastern Raukumara Peninsula: Implications for oil exploration. In New Zealand Petroleum Conference Abstracts. Queenstown, NZ, pp. 29.

McArthur, A.D., and McCaffrey, W.D., 2018, Sedimentary architecture of detached deep-marine canyons: Examples from the East Coast Basin of New Zealand. Sedimentology, doi: 10.1111/sed.12536

McCubbine, J.C., Stagpoole, V., Tontini, F.C., Amos, M., Smith, E., and Winefield, R., 2017, Gravity anomaly grids for the New Zealand region: New Zealand Journal of Geology and Geophysics, v. 60, p. 381–391, doi: 10.1080/00288306.2017.1346692.

Morley, C.K., King, R., Hillis, R., Tingay, M., and Backe, G., 2011, Deepwater fold and thrust belt classification, tectonics, structure and hydrocarbon prospectivity: A review: Earth-Science Reviews, v. 104, p. 41–91, doi: 10.1016/j.earscirev.2010.09.010.

Mortimer, N., 2004, New Zealand's geological foundations: Gondwana Research, v. 7, p. 261–272.

Mortimer, N., Rattenbury, M.S., King, P.R., Bland, K.J., Barrell, D.J.A., Bache, F., Begg, J.G., Campbell, H.J., Cox, S.C., Crampton, J.S., and Edbrooke, S.W., 2014, High-level stratigraphic scheme for New Zealand rocks: New Zealand Journal of Geology and Geophysics, v. 57, p. 402-419.

Mountjoy, J.J., Barnes, P.M., and Pettinga, J.R., 2009, Morphostructure and evolution of submarine canyons across an active margin: Cook Strait sector of the Hikurangi Margin, New Zealand: Marine Geology, v. 260, p. 45–68.

Neef, G., 1992, Turbidite deposition in five miocene, bathyal formations along an active plate margin, North Island, New Zealand: with notes on styles of deposition at the margins of east coast bathyal basins: Sedimentary Geology, v. 78, p. 111–136, doi: 10.1016/0037-0738(92)90116-9.

Nicol, A., and Beavan, J., 2003, Shortening of an overriding plate and its implications for slip on a subduction thrust, central Hikurangi Margin, New Zealand: Tectonics, v. 22, pp. 14.

Nicol, A., and Wallace, L.M., 2007, Temporal stability of deformation rates: Comparison of geological and geodetic observations, Hikurangi subduction margin, New Zealand: Earth and Planetary Science Letters, v. 258, p. 397–413, doi: 10.1016/j.epsl.2007.03.039.

Nicol, A., Van Dissen, R., Vella, P., Alloway, B., and Melhuish, A., 2002, Growth of contractional structures during the last 10 m.y. at the southern end of the emergent Hikurangi forearc basin, New Zealand: New Zealand Journal of Geology and Geophysics, v. 45, p. 365–385, doi: 10.1080/00288306.2002.9514979.

Nicol, A., Mazengarb, C., Chanier, F., Rait, G., Uruski, C., and Wallace, L., 2007, Tectonic evolution of the active Hikurangi subduction margin, New Zealand, since the Oligocene:

Tectonics, v. 26, p. 1–24, doi: 10.1029/2006TC002090.

Noda, A., 2018, Forearc basin stratigraphy and interactions with accretionary wedge growth according to the critical taper concept: Tectonics, v. 37, p. 965-988.Olafiranye, K., Jackson, C.A.-L., and Hodgson, D.M., 2013, The role of tectonics and mass-transport complex emplacement on upper slope stratigraphic evolution: A 3D seismic case study from offshore Angola: Marine and Petroleum Geology, v. 44, p. 196–216, doi: https://doi.org/10.1016/j.marpetgeo.2013.02.016.

Pecher, I.A., Henrys, S.A., Ellis, S., Chiswell, S.M., and Kukowski, N., 2005, Erosion of the seafloor at the top of the gas hydrate stability zone on the Hikurangi Margin, New Zealand: Geophysical Research Letters, v. 32, pp. 4. doi: 10.1029/2005GL024687.

Pettinga, J.R., 1982, Upper Cenozoic structural history, coastal Hawke's Bay, New Zealand: New Zealand Journal of Geology and Geophysics, v. 25, p. 149–191.

Van der Pluijm, B.A., and Marshak, S., 2004, Earth structure: WW Norton & Company, New York, pp. 673.

Prather, B.E., 2003, Controls on reservoir distribution, architecture and stratigraphic trapping in slope settings: Marine and Petroleum Geology, v. 20, p. 529–545.

Raine, J.I., Beu, A.G., Boyes, A.F., Campbell, H., Cooper, R.A., Crampton, J.S., Crundwell, M.P., Hollis, C.J., and Morgans, H.E.G., 2015, Revised calibration of the New Zealand Geological Timescale: NTGT2015/1. Lower Hutt: GNS Science.

Rait, G., Chanier, F., and Waters, D.W., 1991, Landward- and seaward-directed thrusting accompanying the onset of subduction beneath New Zealand: Geology, v. 19, p. 230–233, doi: 10.1130/0091-7613(1991)019<0230:LASDTA>2.3.CO;2.

Reyners, M., 2013, The central role of the Hikurangi Plateau in the Cenozoic tectonics of New Zealand and the Southwest Pacific: Earth and Planetary Science Letters, v. 361, p. 460–468, doi: 10.1016/j.epsl.2012.11.010.

Reyners, M., Eberhart-Phillips, D., and Bannister, S., 2011, Tracking repeated subduction of the Hikurangi Plateau beneath New Zealand: Earth and Planetary Science Letters, v. 311, p. 165–171, doi: 10.1016/j.epsl.2011.09.011.

Spörli, K.B., 1978, Mesozoic tectonics, North Island, New Zealand: Geological Society of America Bulletin, v. 89, p. 415-425.

Spörli, K.B., 1980, New Zealand and oblique-slip margins: tectonic development up to and during the Cainozoic, *in* Ballance, P.F., Reading, H.G. eds., Sedimentation in Oblique-slip Mobile Zones. International Association of Sedimentologists Special Publication, Blackwell Scientific Publications, Oxford, p. 147–170.

Storti, F., and McClay, K., 1995, Influence of syntectonic sedimentation on thrust wedges in analogue models: Geology, v. 23, p. 999–1002.

Totake, Y., Butler, R.W.H., Bond, C.E., and Aziz, A., 2017, Analyzing structural variations along strike in a deep-water thrust belt: Journal of Structural Geology, v. 108, p. 213-229.

Trewick, S.A., and Bland, K.J., 2012. Fire and slice: palaeogeography for biogeography at New Zealand's North Island/South Island juncture: Journal of the Royal Society of New Zealand, v. 42, p. 153-183.

Uruski, C.I., 1997, Post-mortem on Titihaoa-1, Wairarapa: Institute of Geological and Nuclear Sciences science report 97/31, pp. 26.

Vinnels, J.S., Butler, R.W.H., McCaffrey, W.D., and Paton, D.A., 2010, Depositional processes across the Sinú accretionary prism, offshore Colombia: Marine and Petroleum Geology, v. 27, p. 794–809.

Watkins, H., Butler, R.W.H., and Bond, C.E., 2017, Using laterally compatible cross sections to infer fault growth and linkage models in foreland thrust belts: Journal of Structural Geology, v. 96, p. 102–117.

Wells, P., 1989, Burial history of Late Neogene sedimentary basins on part of the New Zealand convergent plate margin: Basin Research, v. 2, p. 145–160, doi: 10.1111/j.1365-2117.1989.tb00032.x.

Wu, S., and Bally, A.., 2000, Slope tectonics— Comparisons and contrasts of structural styles of salt and shale tectonics of the northern Gulf of Mexico with shale tectonics of offshore Nigeria in Gulf of Guinea, *in* Mohriak, W. and Talwani, M. eds., Atlantic rifts and continental margins, American Geophysical Union, Washington, D.C., p. 151–172.

Figure captions

Fig. 1. A) North Island geological map (Heron 2014) and bathymetry (courtesy of NIWA); relative plate motion from Nicol *et al*. (2007). B) Schematic cross-section of the Hikurangi subduction complex, after Nicol *et al*. (2007).

Fig. 2. Tectono-stratigraphy of the East Coast Basin (modified from Bland *et al*. 2015 and Burgreen *et al*. 2016). Regional tectonics adapted from Reyners *et al*. (2013) and Burgreen-Chan *et al*. (2016). New Zealand geological timescale after Raine *et al*. (2015).

Fig. 3. A) Area covered by the PEG14 survey. Bathymetry courtesy of NIWA. Satellite-derived Free-air (offshore) and crustal Bouguer gravity anomalies (onshore) for the East Coast Basin, courtesy of GNS Science. B) Annotated geology and bathymetry map with seismic survey coverage utilised in this study and names of key morphological features. Key to sub-basin and structural high names: Forearc: DaB, Dannevirke Sub-basin; WaB, Wairarapa Sub-basin. Inner portion, emerged: AkB, Akitio Sub-basin; AoH, Aorangi Range; CoH, Coastal Block; MaB, Makara Sub-basin; PoH, Pongaroa Block; PuB, Puketoi Sub-basin; PuH, Puketoi Range; WhB, Whareama Sub-basin. Inner portion, submerged: CoB, Coastal Sub-basin; TiH, Titihaoa Ridge; MdB, Madden Sub-basin; MoT, Motuokura Sub-basin; PaB, Pahaua Trough. Mid portion: OmB, Omakere Sub-basin; PaT, Paoanui Trough; PoT, Porangahau Trough; UrT, Uruti Trough. Outer portion: AoT, Aorangi Trough; AoH, Aorangi Ridge; AkT, Akitio Trough; PuT, Pukehoko Trough; RgH, Rock Garden.

Fig. 4. Non-interpreted (top) and interpreted (bottom) seismic line across the northern zone of the Hikurangi subduction wedge, highlights the variation in structural style and hence morphology of trench-slope sub-basins on this margin from the offshore inner to outer portions. VE, vertical exaggeration.

Fig. 5. Non-interpreted (top) and interpreted (bottom) seismic line across the south-central zone of the Hikurangi subduction wedge, highlights the variation in structural style and morphology of trench-slope sub-basins, Well Titihaoa-1 provides control on trench-slope reflector ages to the Middle Miocene. VE, vertical exaggeration.

Fig. 6. Non-interpreted (top) and interpreted (bottom) seismic line across the southern zone of the Hikurangi subduction wedge, highlights the narrowing of the subduction wedge and limited trench-slope accommodation space. VE, vertical exaggeration.

Fig. 7. A) Non-interpreted seismic line across the northern zone of the Hikurangi subduction wedge with locations of interpreted seismic reflection fill of B) the Madden Sub-basin; C) the Porangahau Trough; D) the Akitio Trough; E) overlay of interpreted seismic units in the Madden Sub-basin; F) overlay of interpreted seismic units in the Porangahau Trough; G) overlay of interpreted seismic units in the Akitio Trough; H) interpreted architectural elements in the Madden Sub-basin; I) interpreted architectural elements in the Porangahau Trough and J) interpreted architectural elements in the Akitio Trough.

Fig. 8. A) Non-interpreted seismic line across the central zone of the Hikurangi subduction wedge with locations of interpreted seismic reflection fill of B) the Coastal Sub-basin; C) the Uruti Trough; D) the Aorangi Trough; E) overlay of interpreted seismic units in the Coastal Sub-basin; F) overlay of interpreted seismic units in the Uruti Trough and G) overlay of interpreted seismic units in the Aorangi Trough. BSR – Bottom Simulating Reflector.

Fig. 9. A) Non-interpreted seismic line across the northern zone of the Hikurangi subduction wedge with locations of interpreted seismic reflection fill of B) the Uruti Trough, Pukehoko Trough and trench; C) overlay of interpreted seismic units in the Uruti Trough, Pukehoko Trough and trench. BSR – Bottom Simulating Reflector.

Fig. 10. Generic model for trench-slope systems. Evolving structural style towards the trench influences the generation of accommodation space, sediment pathways and hence distribution of potential source rocks, reservoir rocks, traps and fluid migration pathways.

Table 1. *Dimensions of sub-basins of the East Coast Basin (cf. Fig. 3)*

Sub-basin name	Length (km)	Width (km)	Infill (m)	Structural style
Dannevirke Sub-basin (DaB)	180	25	3200 (Lee and Begg, 2002)	Forearc, central and north zones
Wairarapa Sub-Basin (WaB)	71	20	2500 (Cape *et al.*, 1990)	Forearc, south zone
Akitio Sub-basin (AkB)	85	14	3600 (Lee and Begg, 2002)	Trench-slope, inner portion, central zone
Makara Sub-Basin (MaB)	72	20	2200 (Lingen & Pettinga, 1980)	Trench-slope, inner portion, north zone
Puketoi Sub-basin (PuB)	60	9	3900 (Lee and Begg, 2002)	Trench-slope, inner portion, central zone
Whareama Sub-basin (WuB)	50	6	4000 (Johnston 1980)	Trench-slope, inner portion, south zone
Coastal Sub-basin (CuB)	50	21	4200	Inner portion, central zone trench-slope
Madden Sub-basin (MdB)	60	15	5128	Trench-slope, inner portion, central zone
Motuokura Trough (MoB)	40	10	3900	Trench-slope, inner portion, north zone
Pahaua Trough (PaB)	30	5	2000 ms^{-1} TWT (IAE-1 survey)	Trench-slope, inner portion, south zone
Omakere Trough (OmB)	70	12	4000	Trench-slope, mid portion, north zone
Porangahau Trough (PoT)	100	15	4750	Trench-slope, mid portion, central zone
Uruti Trough (UrB)	80	13	3020	Trench-slope, mid portion, south zone
Aorangi Trough (AoT)	50	8	1150	Trench-slope, outer portion, south zone
Akitio Trough (AkT)	80	15	1637	Trench-slope, outer portion, central zone
Pukehoko Trough (PuT)	50	10	2950	Trench-slope, outer portion, South zone

Table 2. *Seismofacies of the East Coast Basin*

Unit	Reflector style	Interpretation
Syn-subdutction E (picked from top of Unit D to seafloor in Fig. 4-9)	The uppermost reflectors are typically lower amplitude than Unit D. Reflectors across the subduction wedge show large mounds up to 1 km thick and up to 15 km wide that form distinctive geometries (Fig. 5). On the subducting plate, low amplitude, typically parallel reflectors are cut by lenticular features kilometres wide and hundreds of meteres deep, with associated sediment waves (Fig. 6).	The mounded geometries in the inner portion are interpreted as contourite drift deposits (*sensu* Faugères *et al*. 1999). On the Pacific Plate the Hikurangi Channel becomes apparent, the general reduction in amplitude and occurrence of sediment waves within the reflectors may indicate that a substantial volume of siliciclastic material was provided to the foreland, both as overbank to the channel and from other transverse sediment conduits.
Syn-subdutction D (picked from top of Unit C top unit D)	Normally conformable over Unit C are higher amplitude, often continuous reflectors. Within the subduction wedge, they may be seen to prograde from the west, often developing over the tops of structures, but with overall wedge-shaped geometries (Fig. 4). In the outer portion of the wedge, they may continue to fill sub-basins onlapping their margins (Fig. 7). In the trench, this interval is the last to onlap and entirely truncate against the Hikurangi Plateau (Fig. 5).	This is interpreted to represent several events in the basin history. The prograding wedge apparent in the inner portion is interpreted to represent a general seaward progradation of the sedimentary system as the North Island developed and the Coastal Ranges grew, elevating the innermost portion of the wedge (Bland *et al*. 2004). Changes in ocean circulation and the development of contour currents (Carter *et al*. 1996) may explain the change in reflector style further offshore.
Syn-subdutction C (picked from top of Unit B top unit C)	Following a tilt of several degrees, Unit C is relatively low amplitude reflectors imaged on the subducting plate and onlapping Unit B (Fig. 5). Lenticular incisions become common within the reflectors. Within the subduction wedge, relatively low amplitude, often chaotic, reflectors can also seen within the sub-basins and correspond to the Upper Miocene interval of Titihaoa-1 and Tawatawa-1.	Geometries within these units indicate the development of siliciclastic submarine units, whilst chaotic reflectors are interpreted as MTCs. This tilt, the decrease in accoustic impedance, the prominance of MTCs, of geobodies with geometries of submarine channels and of lobes may be correlated with the renewed phase of collision, driving higher deformation rates and expulsion of siliciclastic material offshore (Bland *et al*. 2015)
Syn-subdutction B (picked from top of Unit A top unit B)	Above another landward tilt and truncation of Unit A, a series of relatively continuous, high amplitude reflectors can be seen on the Pacific Plate, which onlaps against the Hikurangi Plateau (Fig. 5). Within the subduction wedge, high amplitude reflectors can be seen within the lower portion of the fill of some of the extensive sub-basins, such as the Porangahau Trough (Fig. 8).	This interval coincides with the deepest well penetration in the wedge: the well Titihaoa-1. This well terminated in the lower middle Miocene, with a marl lithology (Uruski 1997), which may indicate a period of quiescence on the margin, leading to the higher amplitude, potentially calcareous deposits.
Syn-subdutction A (picked from top of Pre-subduction reflectors top unit A)	Occurring above continuous, high amplitude reflectors of the pre-subduction interval. A regional tilt of strata towards the west is followed by the occurrence of relatively low amplitude, often discontinuous reflectors on the subducting plate (Fig. 5). Within the subduction wedge, these reflectors are often heavily deformed, but can occasionally be imaged in the basal fill of trench-slope sub-basins (Fig. 7).	These are interpreted to represent the first syn-subduction strata of the Neogene subduction event (Fig. 2). This strata may be diachronous across the region, with the earliest effects of the deformation being recorded in the inner portion by lower Miocene siliciclastic sediment. However, even the deposits in the Hikurangi Trough may represent Miocene deposits, as siliciclastic material is first reported in the IODP well 1124 on the Hikurangi Plateau in the Lower Miocene (Joseph *et al*. 2004).

Table 3. *Summary of morphostructural elements of the East Coast Basin fold and thrust belt*

SUBDUCTION DOMAINS & morphological portions	Morphological elements & *boundaries*	Location	Thrust tectonics Model	Physical locations in New Zealand	Information from literature	From gravity data	From bathymetry & topography data	From seismic data
FOREARC BASIN	Forearc basin *End of Ranges*	Onshore Emerged	Thick-skinned	Dannevirke Sub-basin (DaB) Wairarapa Sub-basin (WaB)	Structural depression between the North Island axial ranges and the subduction wedge	Positive anomalies, negative closer to North Island axial ranges	20-25 km width 70-180 km length	N/A
SUBDUCTION WEDGE Inner portion	Trench-slope break *Coastal Ranges*	Onshore Emerged	Thick-skinned	Akitio Sub-basin (AKB) Makara Sub-basin (MaB) Puketoi Sub-basin (PuB) Whareama Sub-basin (WhB) Aorangi Range (AoH) Coastal Block (CoH) Pongaroa Block (PoH) Puketoi Range (PuH)	Highly deformed, thickened basement of strata previously accreted on Gondwana margin (pre-Hikurangi subduction) Isolated strip of syn-subduction Neogene strata visible onshore Neogene trench-slope basins and shelf strata	Positive anomalies Largely filled troughs Underlying thickened crust of ~28-30 km	10-20 km width 60-85 km length Fault spacing 10s kilometres Preserved remnants of trench-slope sub-basins	*Structures* Majority of high angle, over-steepened faults. with connections to deeper structures Presence of back thrusts *Trench-slope Infill* <3 to over 5 km of syn-subduction strata Asymmetrical, complex infill with multiple unconformities, of faulted and folded strata Heterolithic infill: MTC development *Basement* Acoustic basement of pre-subduction strata at 4 to 8 km depth Occasional floating rafts, coherent reflectors *Deformation style* Reactivation zone: reactivation of older structures, and strata remobilization
	Continental Shelf *Wairarapa Shelf*	Offshore Submerged	Thick-skinned	Coastal Sub-basin (CoB) Madden Sub-basin (MdB) Motuokura Sub-basin (MoT) Pahaua Trough (PaB)			10-20 km width 60-85 km length Trench-parallel ridges, generally smooth with up to 100 m relief	
SUBDUCTION WEDGE	*Shelf Break* Continental		Thick-	Omakere Sub-basin (OmB)	Imbricated foundation of pre-	Mixed anomalies:	10-15 km width	*Structures* Steep, thrust fault detachments, with connection to deeper structures

Mid portion	Slope *Imbricate fan*	Offshore Submerged	skinned	Paoanui Trough (PaT) Porangahau Trough (PoT) Uruti Trough (UrT)	subduction rocks Thrust faults connect to deeper structures Out-of-sequence thrusting Neogene trench-slope basins	+/- neutral Troughs developing and filling Underlying thickened crust of ~28-30 km	70-100 km length Narrow troughs with steep ridges due to seamount subduction in outer portion, widening troughs otherwise Fill to spill troughs often demonstrating bypassing channels and canyons	Out-of-sequence thrusts Developing detachment folds *Trench-slope Infill* < 5 km of syn- subduction strata Relatively symmetrical infill for lower part, pinching out on sub-basin margin, including interspersed chaotic reflectors i.e. MTCs Asymmetrical, complex infill with multiple unconformities in the upper part *Deformation style* Imbricate fan development, except if subduction of seamount occurred: triggers antiformal stack development
SUBDUCTION WEDGE Outer portion	*Antiformal stack* Accretionary Prism *sensu stricto*	Offshore Submerged	Thin-skinned	Aorangi Trough (AoT) Akitio Trough (AkT) Pukehoko Trough (PuT) Rock Garden (RgH)	Widely spaced propagating thrusts and frontal folds Recent trench-slope basins with syn-subduction strata	Essentially negative anomalies Rare positive anomalies highlights subducted seamount positions Base-of-slope structures and proto-troughs developing Underlying oceanic crust up to ~12 km	5-10 km width Up to 80 km length Very narrow & elongated asymmetrical basin geometries Moderate to high ridge rugosity, up to 1 km of relief	*Structures* Highly variable from south to north Proto-frontal fold system or already developing thrusts with associated fault propagation folds *Infill* Developing into trench-slope basins Isolated depocentres of <1 to 3 km of syn-subduction strata, relatively coherent, undeformed strata Smooth transition with pre-subduction strata Distinct from accreted strata: deformed and truncated by faults *Deformation style* Accretionary Prism *sensu stricto*
SUBDUCTION TROUGH	*Deformation Front* Trench Floor	Offshore Submerged	-	Hikurangi Trough (HiT)	Trench floor Proto-thrust zone of ~10-15 km in front of deformation front Accreting sediments	Negative anomalies Trench floor location	20 km (North) to over 90 km (South) trench floor width No trench-slope basins Hikurangi trench axial channel	*Structures* Proto-thrust zone of ~10-15 km in front of deformation front *Infill* Up to 5 km of syn-kinematic strata Accreted strata Hikurangi channel and paleo-Hikurangi channel infill

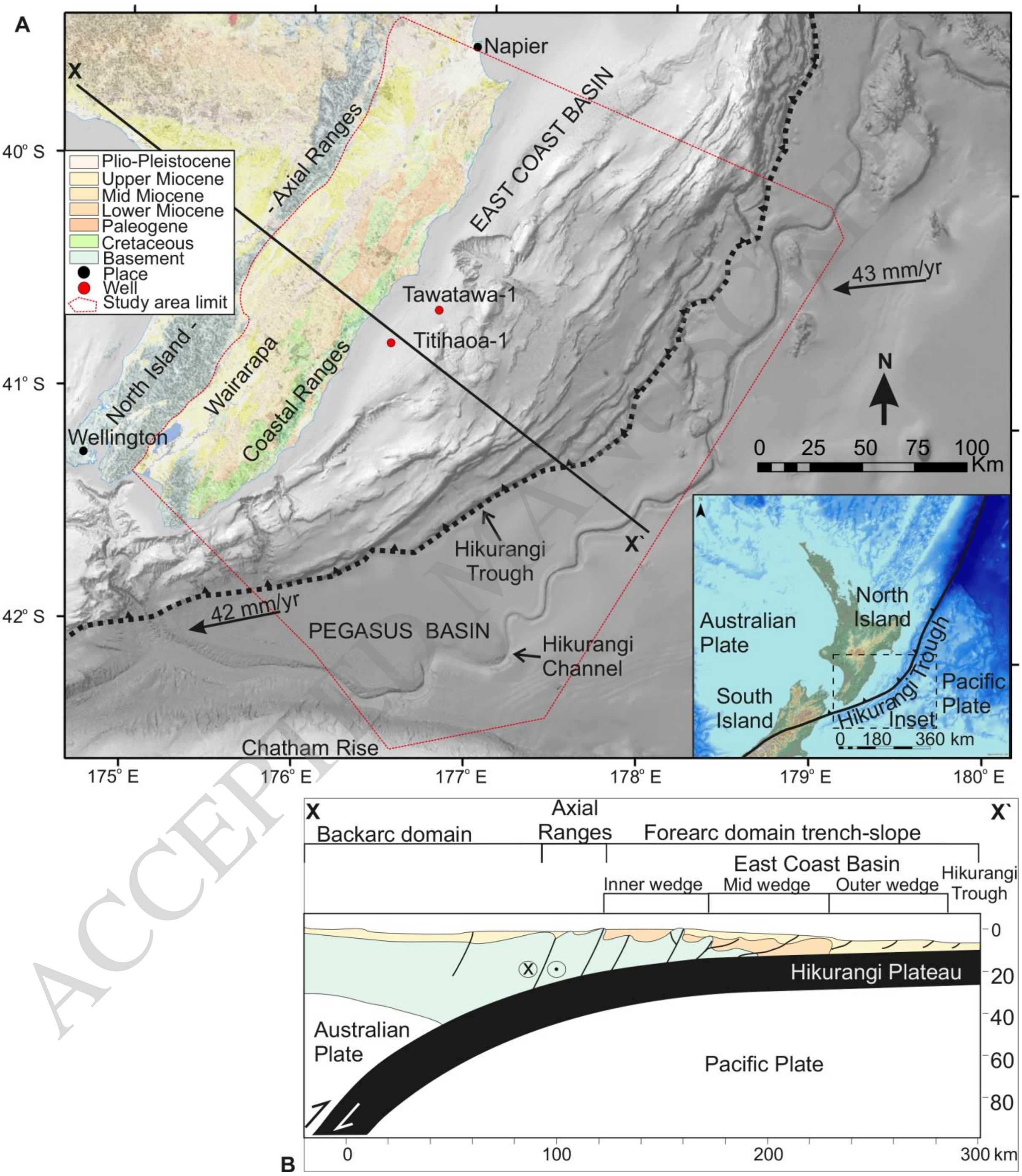
A
X
Napier
EAST COAST BASIN
- Axial Ranges
Plio-Pleistocene
Upper Miocene
Mid Miocene
Lower Miocene
Paleogene
Cretaceous
Basement
Place
Well
Study area limit
40° S
41° S
42° S
Tawatawa-1
Titihaoa-1
43 mm/yr
N
0 25 50 75 100 Km
North Island -
Wairarapa
Coastal Ranges
Wellington
Hikurangi Trough
X`
42 mm/yr
PEGASUS BASIN
Hikurangi Channel
Chatham Rise
Australian Plate
North Island
South Island
Hikurangi Trough
Pacific Plate
Inset
0 180 360 km
175° E
176° E
177° E
178° E
179° E
180° E
X
X`
Backarc domain
Axial Ranges
Forearc domain trench-slope
East Coast Basin
Inner wedge
Mid wedge
Outer wedge
Hikurangi Trough
Hikurangi Plateau
Australian Plate
Pacific Plate
0
20
40
60
80
0
100
200
300 km
B

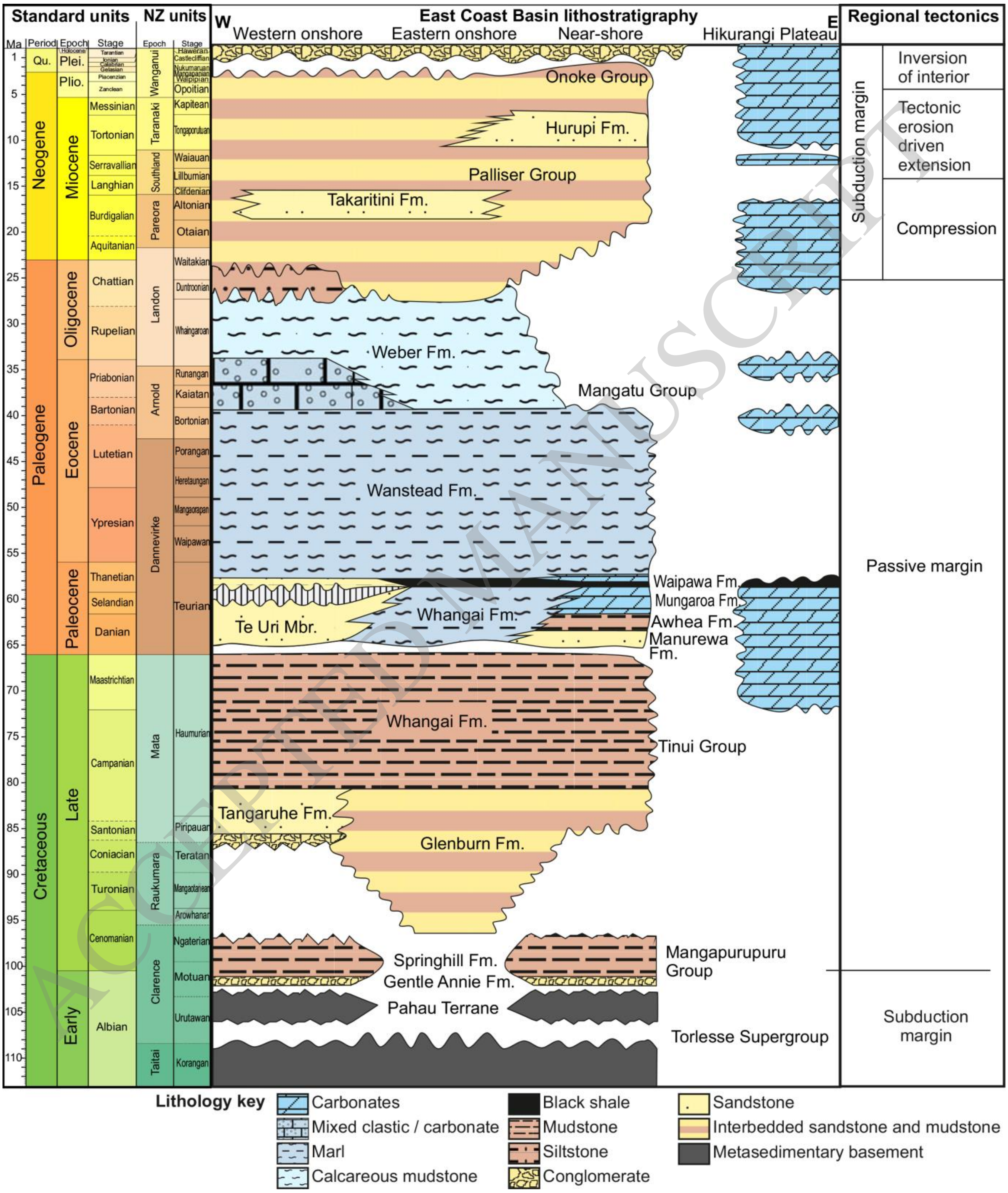

Standard units
NZ units
East Coast Basin lithostratigraphy
W
Western onshore
Eastern onshore
Near-shore
Hikurangi Plateau
E
Regional tectonics
Ma
Period
Epoch
Stage
Qu.
Plei.
Plio.
Neogene
Miocene
Paleogene
Oligocene
Eocene
Paleocene
Cretaceous
Late
Early
Zanclean
Messinian
Tortonian
Serravallian
Langhian
Burdigalian
Aquitanian
Chattian
Rupelian
Priabonian
Bartonian
Lutetian
Ypresian
Thanetian
Selandian
Danian
Maastrichtian
Campanian
Santonian
Coniacian
Turonian
Cenomanian
Albian
Wanganui
Taranaki
Southland
Pareora
Landon
Arnold
Dannevirke
Mata
Raukumara
Clarence
Taitai
Haweran
Castlecliffian
Nukumaruan
Mangapanian
Waipipian
Opoitian
Kapitean
Tongaporutuan
Waiauan
Lillburnian
Clifdenian
Altonian
Otaian
Waitakian
Duntroonian
Whaingaroan
Runangan
Kaiatan
Bortonian
Porangan
Heretaungan
Mangaorapan
Waipawan
Teurian
Haumurian
Piripauan
Teratan
Mangaotanean
Arowhanan
Ngaterian
Motuan
Urutawan
Korangan
Onoke Group
Hurupi Fm.
Palliser Group
Takaritini Fm.
Weber Fm.
Mangatu Group
Wanstead Fm.
Waipawa Fm.
Mungaroa Fm.
Whangai Fm.
Te Uri Mbr.
Awhea Fm.
Manurewa Fm.
Whangai Fm.
Tinui Group
Tangaruhe Fm.
Glenburn Fm.
Springhill Fm.
Gentle Annie Fm.
Mangapurupuru Group
Pahau Terrane
Torlesse Supergroup
Subduction margin
Inversion of interior
Tectonic erosion driven extension
Compression
Passive margin
Subduction margin
Lithology key
Carbonates
Mixed clastic / carbonate
Marl
Calcareous mudstone
Black shale
Mudstone
Siltstone
Conglomerate
Sandstone
Interbedded sandstone and mudstone
Metasedimentary basement

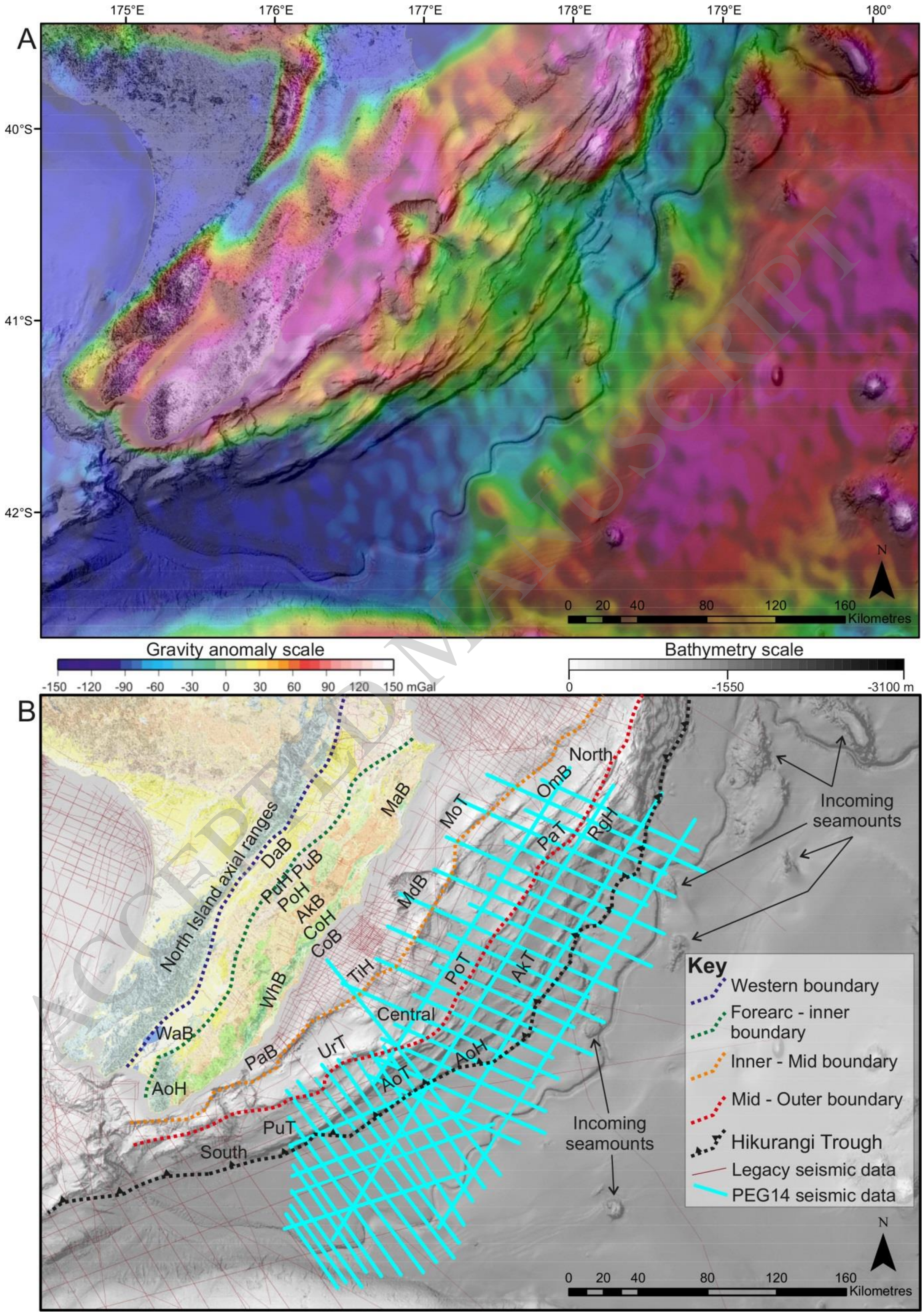

175°E
176°E
177°E
178°E
179°E
180°
A
40°S
41°S
42°S
0 20 40 80 120 160 Kilometres
Gravity anomaly scale
-150 -120 -90 -60 -30 0 30 60 90 120 150 mGal
Bathymetry scale
0 -1550 -3100 m
B
North Island axial ranges
DaB
PuH PuB
PoH
AkB
CoH
CoB
MaB
MoT
MdB
TiH
WhB
WaB
AoH
PaB
UrT
Central
PoT
AkT
OmB
PaT
RgH
North
AoT
AoH
PuT
South
Incoming seamounts
Incoming seamounts
Key
Western boundary
Forearc - inner boundary
Inner - Mid boundary
Mid - Outer boundary
Hikurangi Trough
Legacy seismic data
PEG14 seismic data
0 20 40 80 120 160 Kilometres

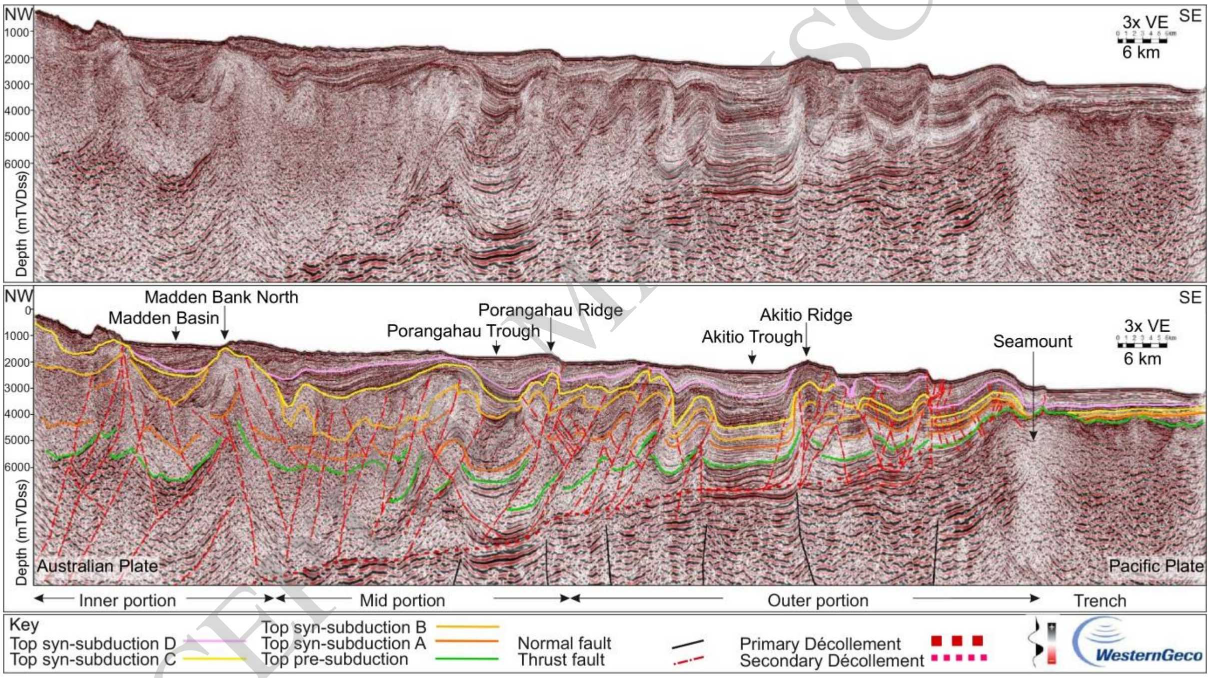

NW
SE
3x VE
6 km
Depth (mTVDss)
1000
2000
3000
4000
5000
6000
Madden Bank North
Madden Basin
Porangahau Ridge
Porangahau Trough
Akitio Ridge
Akitio Trough
Seamount
Australian Plate
Pacific Plate
Inner portion
Mid portion
Outer portion
Trench
Key
Top syn-subduction D
Top syn-subduction C
Top syn-subduction B
Top syn-subduction A
Top pre-subduction
Normal fault
Thrust fault
Primary Décollement
Secondary Décollement
WesternGeco

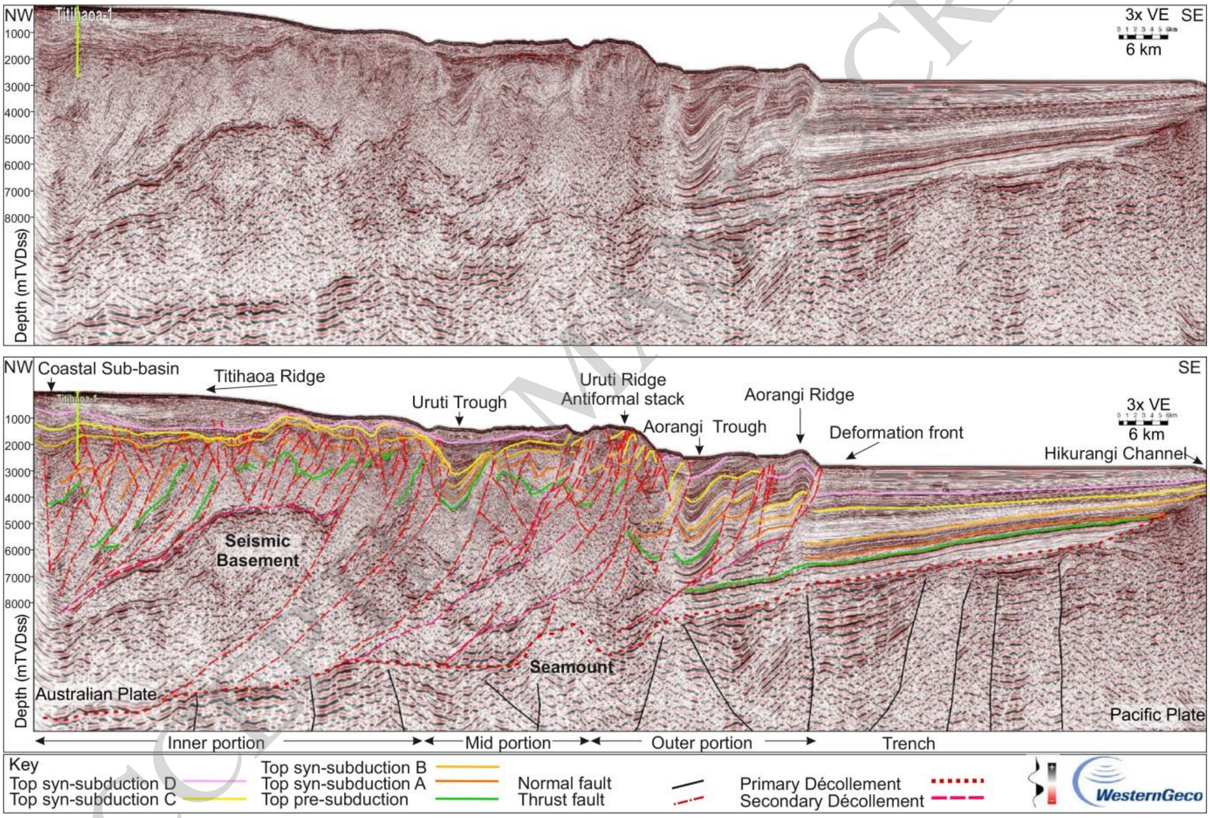

NW
Titihaoa-1
3x VE
SE
6 km
1000
2000
3000
4000
5000
6000
7000
8000
Depth (mTVDss)
NW
Coastal Sub-basin
Titihaoa Ridge
Uruti Trough
Uruti Ridge
Antiformal stack
Aorangi Ridge
Aorangi Trough
Deformation front
Hikurangi Channel
SE
Seismic Basement
Seamount
Australian Plate
Pacific Plate
Inner portion
Mid portion
Outer portion
Trench
Key
Top syn-subduction D
Top syn-subduction C
Top syn-subduction B
Top syn-subduction A
Top pre-subduction
Normal fault
Thrust fault
Primary Décollement
Secondary Décollement
WesternGeco

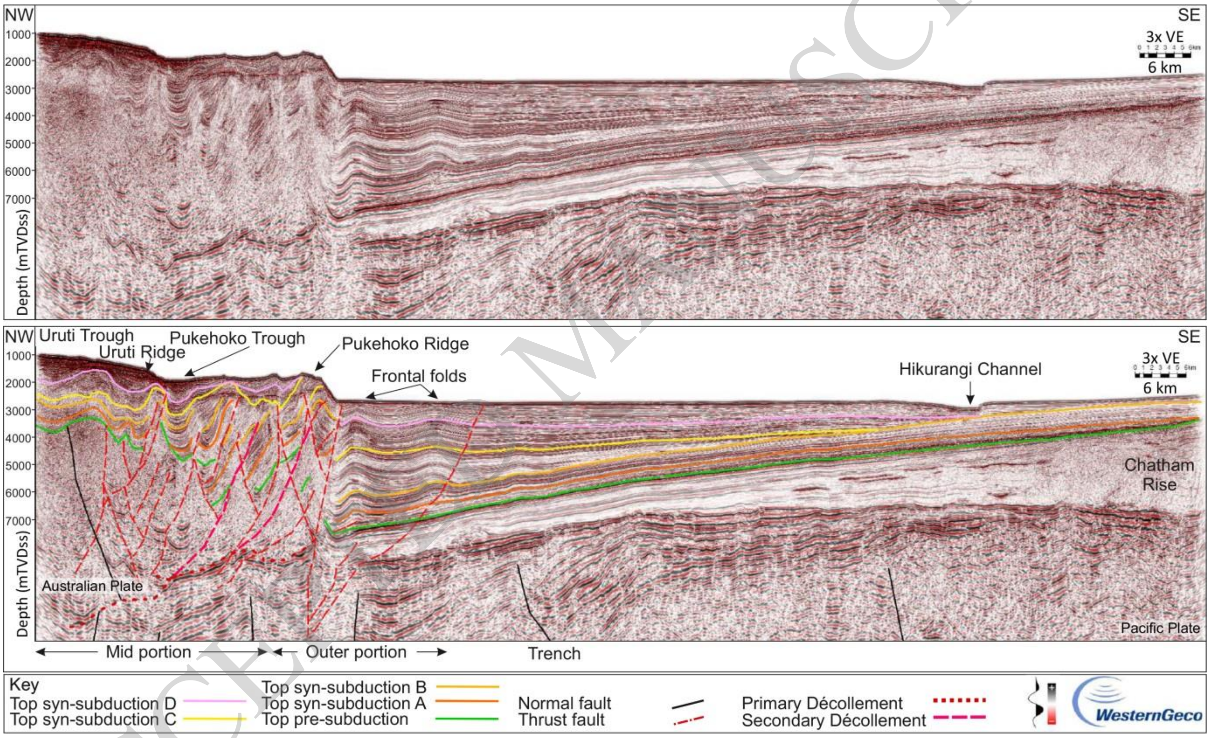

NW
SE
3x VE
6 km
Depth (mTVDss)
Uruti Trough
Uruti Ridge
Pukehoko Trough
Pukehoko Ridge
Frontal folds
Hikurangi Channel
Chatham Rise
Australian Plate
Pacific Plate
Mid portion
Outer portion
Trench
Key
Top syn-subduction D
Top syn-subduction C
Top syn-subduction B
Top syn-subduction A
Top pre-subduction
Normal fault
Thrust fault
Primary Décollement
Secondary Décollement
WesternGeco

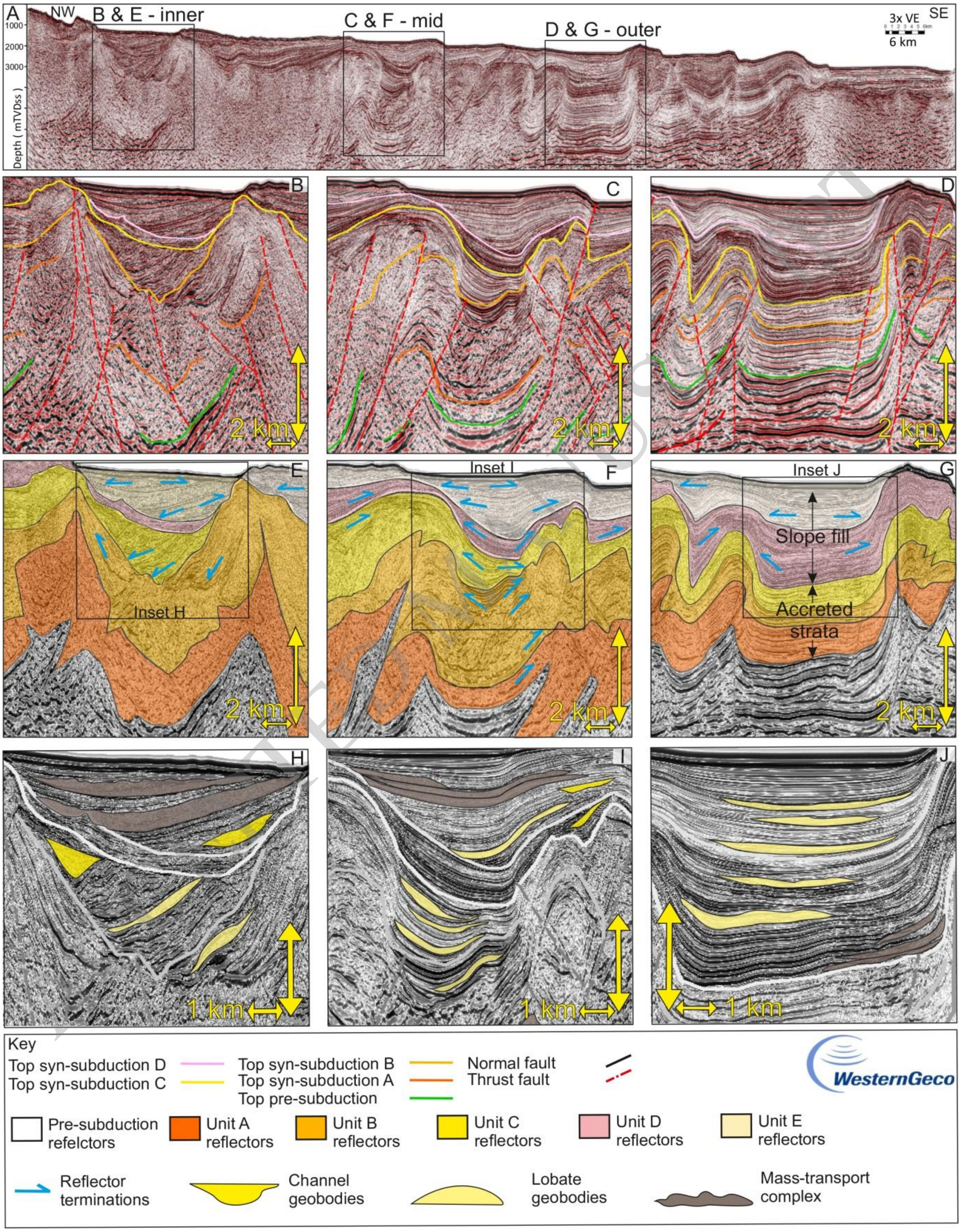
A
NW
B & E - inner
C & F - mid
D & G - outer
3x VE
SE
6 km
1000
2000
3000
Depth (mTVDss)
B
C
D
2 km
E
F
G
Inset H
Inset I
Inset J
Slope fill
Accreted strata
H
I
J
1 km
Key
Top syn-subduction D
Top syn-subduction C
Top syn-subduction B
Top syn-subduction A
Top pre-subduction
Normal fault
Thrust fault
WesternGeco
Pre-subduction refelctors
Unit A reflectors
Unit B reflectors
Unit C reflectors
Unit D reflectors
Unit E reflectors
Reflector terminations
Channel geobodies
Lobate geobodies
Mass-transport complex

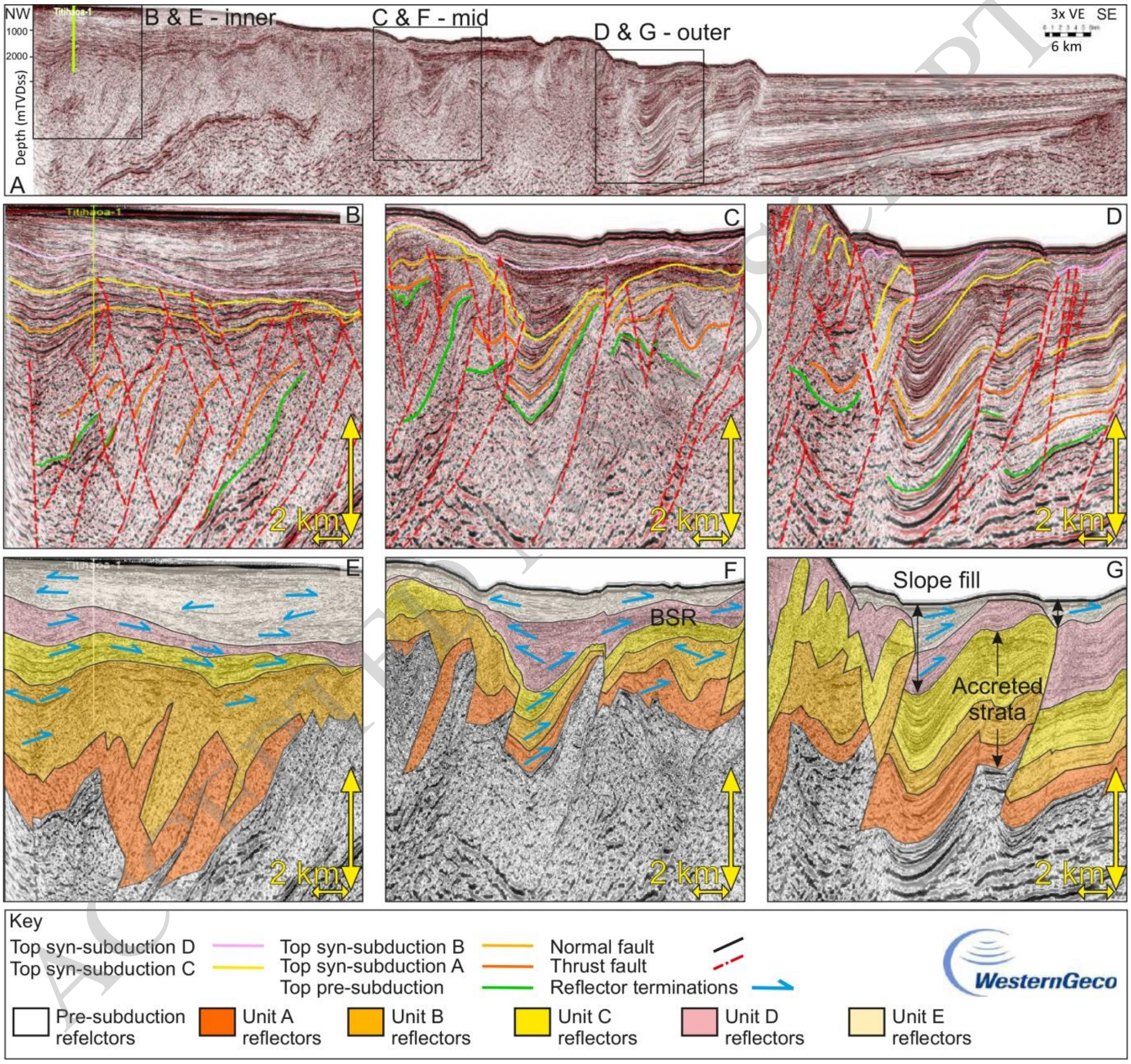
NW
SE
3x VE
6 km
B & E - inner
C & F - mid
D & G - outer
Titihaoa-1
1000
2000
Depth (mTVDss)
A
B
C
D
E
F
G
2 km
BSR
Slope fill
Accreted strata
Key
Top syn-subduction D
Top syn-subduction C
Top syn-subduction B
Top syn-subduction A
Top pre-subduction
Normal fault
Thrust fault
Reflector terminations
Pre-subduction refelctors
Unit A reflectors
Unit B reflectors
Unit C reflectors
Unit D reflectors
Unit E reflectors
WesternGeco

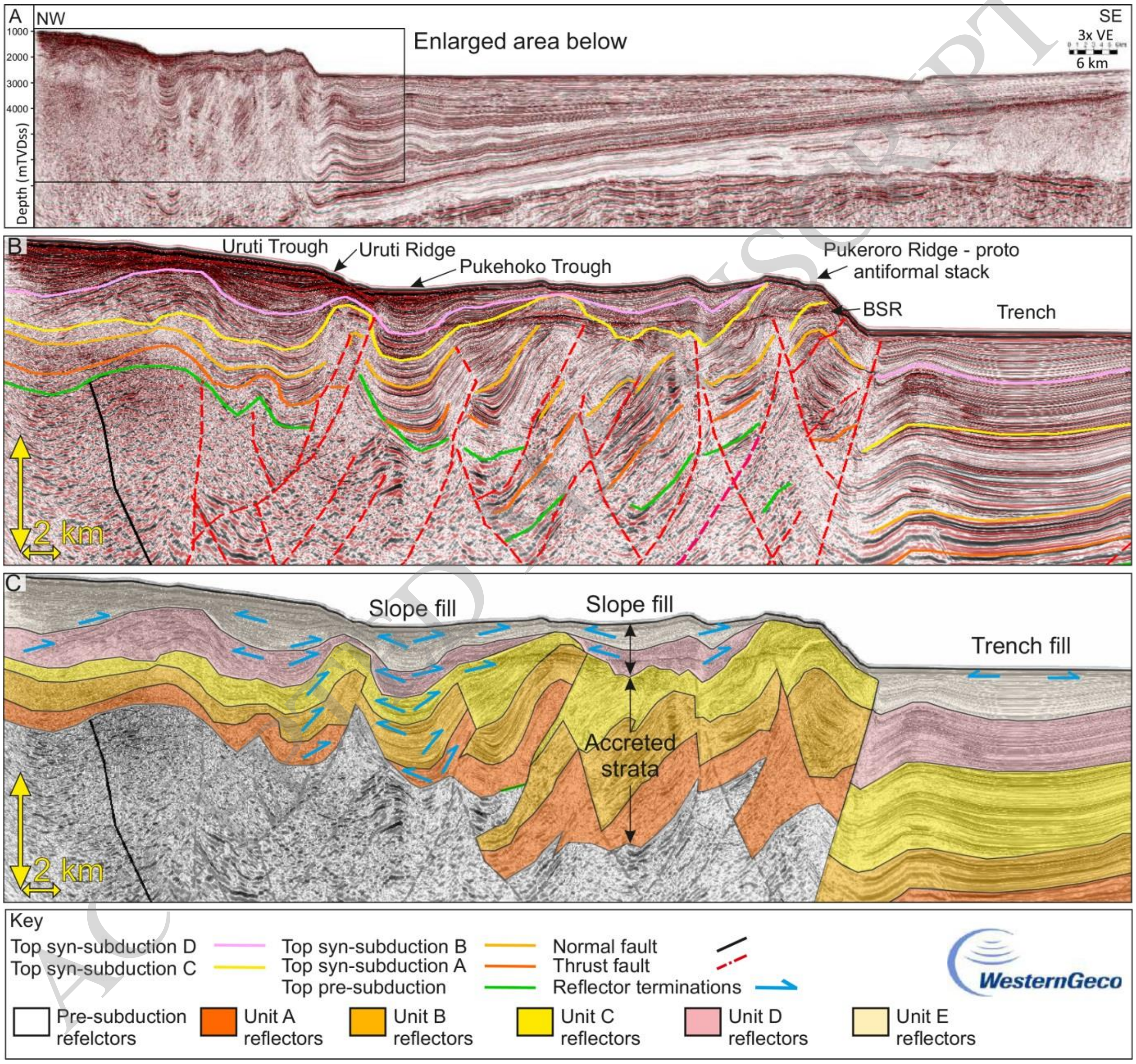
A
NW
SE
Enlarged area below
3x VE
6 km
1000
2000
3000
4000
Depth (mTVDss)
B
Uruti Trough
Uruti Ridge
Pukehoko Trough
Pukeroro Ridge - proto antiformal stack
BSR
Trench
2 km
C
Slope fill
Slope fill
Trench fill
Accreted strata
2 km
Key
Top syn-subduction D
Top syn-subduction C
Top syn-subduction B
Top syn-subduction A
Top pre-subduction
Normal fault
Thrust fault
Reflector terminations
WesternGeco
Pre-subduction refelctors
Unit A reflectors
Unit B reflectors
Unit C reflectors
Unit D reflectors
Unit E reflectors

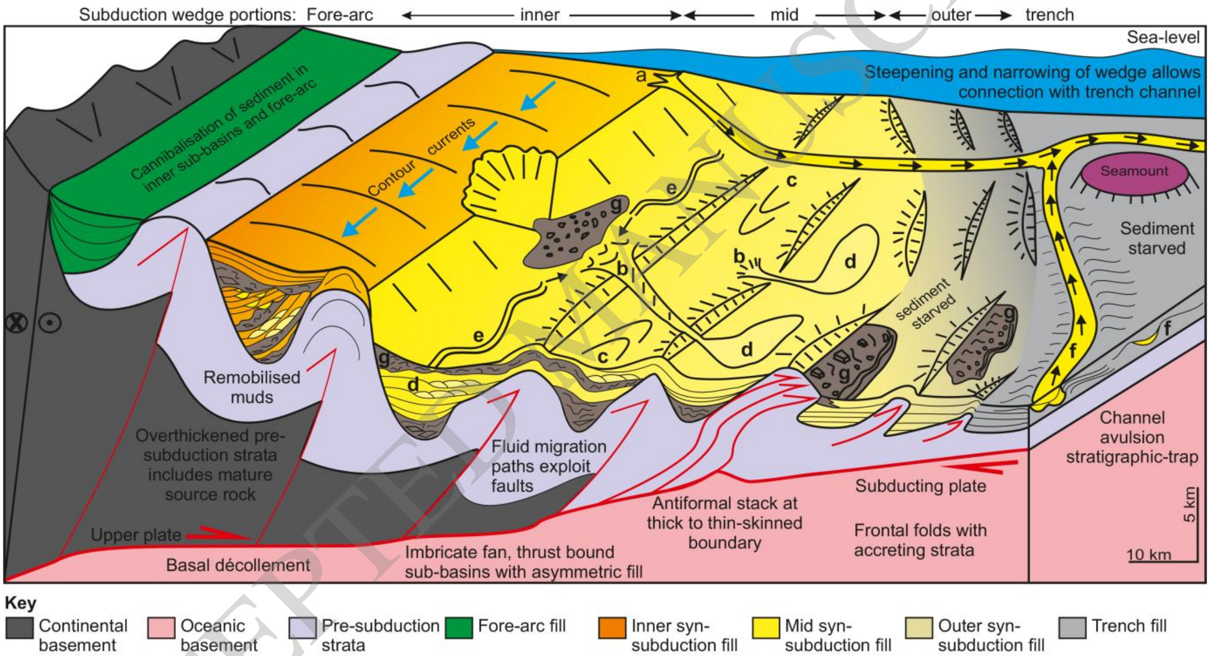

Fill elements: a) Shelf attached canyon; b) Detached canyon; c) Migratory lobe; d) Terminal lobe; e) Trough-axial channel; f) Trench-axial channel; g) MTC